Supporting Information

# Mechanoredox Catalyzed Cationic RAFT Polymerization via Perfluorinated Anion Assistance for High-Molecular-Weight Polymers

Longfei Zhang, [a] Ziye Ren, [a] Kai Chen, [a] Huanyu Lei *[a] and Zhao Wang *[a]

[a]State and Local Joint Engineering Laboratory for Novel Functional Polymeric Materials, Jiangsu Key Laboratory of Advanced Functional Polymer Design and Application, Suzhou Key Laboratory of Macromolecular Design and Precision Synthesis, College of Chemistry, Chemical Engineering and Materials Science, Soochow University, Suzhou 215123, China. E-mail: wangzhao@suda.edu.cn; leihy@suda.edu.cn

## Table of Contents

## Materials

Isobutyl vinyl ether (IBVE; 99%, TCI), n-butyl vinyl ether (NBVE; 99%, TCI), n-propyl vinyl ether (NPVE, 97%, TCI), ethyl vinyl ether (EVE, 98%, TCI), cyclohexyl vinyl ether (CyVE, 98%, TCI), 2-chloroethyl vinyl ether (Cl-EVE, 99%, Sigma-Aldrich), dihydrofuran (DHF, 98%, TCI) were filtered through a plug of neutral alumina to remove inhibitors prior to use. *S*-(trifluoromethyl)dibenzothiophenium tetrafluoroborate ($CF_3$ reagent a, 97%), *S*-(trifluoromethyl)dibenzothiophenium tetrafluoroborate ($CF_3$ reagent b, 97%), *S*-(trifluoromethyl)thionitronium triflate ($CF_3$ reagent c, 97%) were purchased from Shanghai Aladdin Biochemical Technology Co., Ltd. Hydrogen chloride ether solution (2.0 M HCl in $Et_2O$) was purchased from Zhoushan Aike Biological Technology Co., Ltd. Anhydrous dichloromethane (DCM, 99%, TCI), sodium diethyldithiocarbamate (98%, J&K), sodium tetrafluoroborate ($NaBF_4$, 98%, TCI), sodium hexafluorophosphate ($NaPF_6$, 98%, J&K), sodium hexafluoroantimonate ($NaSbF_6$, 98%, J&K), sodium hexafluoroarsenate ($NaAsF_6$, 98%, MERYER )were used as received. All ball-milling (BM) experiments were carried out in a Retsch Mixer Mill (MM 400) ball mill instrument using 1.5 mL stainless-steel grinding jars equipped with a single 5 mm stainless-steel grinding ball.

## Characterization

$^1$H NMR and $^{13}$C NMR were recorded on a BRUKER AVANCE NEO 400MHz nuclear magnetic resonance instrument by using $CDCl_3$ as solvent and tetramethylsilane as the internal standard. The number-average molecular weight ($M_{n,}$) and dispersity ($Đ$) of the obtained polymers were determined by a TOSOH HLC-8320 SEC equipped with a TSK gel Multipore HZ-N (3) 4.6 × 150 mm column at 40 ℃. THF served as the eluent with a flow rate of 0.35 mL·min$^{-1}$. SEC samples were injected using the TOSOH HLC-8320 SEC plus autosampler. The number-average molecular weight ($M_n$) and dispersity ($Đ$) were calibrated with PS standards. GC-MS analysis was performed using an Agilent 5977C GC/MSD single quadrupole mass spectrometer coupled to an Agilent 8860 gas chromatograph.

Matrix-assisted laser desorption/ionization time-of-flight mass spectrometry (MALDI-TOF MS) was measured on an UltrafleXtreme III MALDI-TOF mass spectrometer (Bruker Daltonics, Germany) The matrix was trans-2-[3-(4-tert-butylphenyl)-2-methyl-2-propenylidene]-malononitrile (DCTB) for PMMA, the additive salt was $CF_3COONa$. Samples were tested in linear mode. And the data analysis was conducted with Bruker's Flex Analysis software.

## Synthetic and Experimental Procedures

### Experimental procedure for synthesis of chain transfer agent S-1-isobutoxyethyl *N*, *N*-diethyl dithiocarbamate (DTCB)

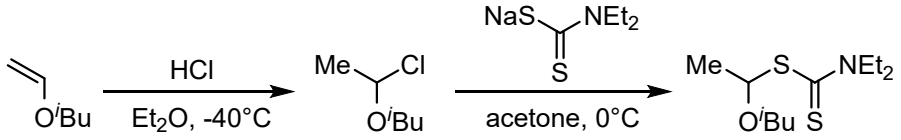


DTCB were synthesized according to the reported method.[1, 2] In a flame dried flask, 2.6 mL isobutyl vinyl ether (IBVE, 20 mmol) was added dropwise to 10 mL hydrogen chloride ether solution (2M, 20 mmol) over 10 min at -40 ℃ and stirred for 3 h to prepare IBVE-HCl adduct. Then, the addition product was slowly dripped into the solution of sodium diethyldithiocarbamate trihydrate (5.4 g, 24 mmol) in acetone (100mL) at 0 °C. Stirring was continued for 1.5 h at 0 °C, followed by 1.5 hours at room temperature. The solvent was removed by rotary evaporation. The crude product was dissolved in 60 mL EA, and washed with saturated sodium bicarbonate ($NaHCO_3$) and sodium chloride (NaCl). The solvent was removed under reduced pressure. The residue was further purified by column chromatography eluting with a solvent mixture of hexane: ethyl acetate (gradient from 10:0 to 9.5:0.5) to afford the compound as light oil (4.1 g, 16.4 mmol, 84% yield).

$^1$H NMR ($CDCl_3$, 400 MHz, δ, ppm): 5.89 (q, 1 H), 4.03 (m, 2 H), 3.75 (m, 2 H), 3.47 (dd, 1 H), 3.34 (dd, 1 H), 1.85 (m, 1 H), 1.73 (d, 3 H), 1.28 (dt, 6 H).

$^{13}$C NMR ($CDCl_3$, 100 MHz, δ, ppm): 195.0, 91.6, 76.0, 48.7, 46.8, 28.3, 23.5, 19.4, 12.6, 11.7.

### Experimental procedure for synthesis of initiators containing different counterions through ion pair replacement

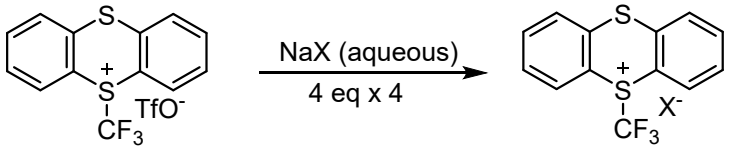


(X$^-$: $BF_4^-$, $PF_6^-$, $AsF_6^-$, $SbF_6^-$)

As an illustrative example, the synthesis of TT-$CF_3^+$ $BF_4^-$ was conducted under air condition.[3] Initially, 1 g *S*-(trifluoromethyl) thionitronium triflate (TT-CF3$^+$ TfO$^-$, 2.3 mmol ) was dissolved in 20 mL DCM. Concurrently, 4 g $NaBF_4$ (36.4 mmol) was dissolved in 80 mL deionized water, and this solution was divided into four equal portions. The dichloromethane solution was washed four times with the $NaBF_4$ aqueous solution, followed by drying with anhydrous $Na_2SO_4$. The mixture was then filtered, and the solvent was removed under reduced pressure to yield a white solid product (TT-$CF_3^+$ $BF_4^-$, 0.75 g, 88 % yield). The product was characterized by $^{19}$F NMR spectroscopy using acetone-d6. Notably, TT-$CF_3^+$ $SbF_6^-$ did not exhibit a signal peak corresponding to $SbF_6^-$, while the disappearance of the $TfO^-$ signal peak confirmed the

successful ion pair replacement.
TT-$CF_3^+$ $TfO^-$ $^{19}F$ NMR (acetone-d6, 376 MHz, δ, ppm): -51.12, -78.43.
TT-$CF_3^+$ $BF_4^-$ $^{19}F$ NMR (acetone-d6, 376 MHz, δ, ppm): -50.66, -149.67, -149.66.
TT-$CF_3^+$ $PF_6^-$ $^{19}F$ NMR (acetone-d6, 376 MHz, δ, ppm): -50.56, -70.45, -72.34.
TT-$CF_3^+$ $AsF_6^-$ $^{19}F$ NMR (acetone-d6, 376 MHz, δ, ppm): -51.08, -62.20, -64.68, -67.15; -69.62.
TT-$CF_3^+$ $SbF_6^-$ $^{19}F$ NMR (acetone-d6, 376 MHz, δ, ppm): -51.86.

**Experimental procedure for mechano-cRAFT polymerization of IBVE under air or Ar**

Under air conditions (relative humidity 40%-50%), the initiator $[CF_3]^+$ $[X]^-$ (0.003 mmol) and 5 mg $MoS_2$ (0.03 mmol, 1.6 wt %) were added to a 1.5 mL stainless steel grinding jar containing a 5 mm diameter ball. Subsequently, 50 μL anhydrous DCM (LAG = 0.2 μL/mg), 2.1 mg DTCB (0.008 mmol) and 250 mg IBVE (2.5 mmol) were added and closed under air. The grinding jar was then placed in the MM400 ball mill and milled at 30 Hz for designated time. Polymerization was quenched with 5% $Et_3N$ in MeOH, and diluted with $CHCl_3$. The solution was centrifuged to remove the $MoS_2$, the supernatant was collected and analyzed by $^1H$ NMR spectroscopy and GPC.
In an argon-filled glove box, the initiator $[CF_3]^+$ $[X]^-$ (0.003 mmol) and 2 mg $MoS_2$ (0.01 mmol, 0.7wt %) were added to a 1.5 mL stainless steel grinding jar containing a 5 mm diameter ball. Subsequently, 10 μL anhydrous DCM (LAG = 0.04 μL/mg), 2.1 mg DTCB (0.008 mmol) and 250 mg IBVE (2.5 mmol) were added, and the grinding jar was closed. The grinding jar was then removed from the glove box and placed in the MM400 ball mill and milled at 30 Hz for designated time. Polymerization was quenched with 5% $Et_3N$ in MeOH, and diluted with $CHCl_3$. The solution was centrifuged to remove the $MoS_2$, the supernatant was collected and analyzed by $^1H$ NMR spectroscopy and GPC.

**Simulation details:**

The density functional theory (DFT) calculation was performed as implemented in Gaussian G16 program package to get a clear understanding about the interaction between the anions ($TfO^-$, $BF_4^-$, $AsF_6^-$) and cations. The optimized geometry was calculated by the dispersion-corrected density functional theory (DFT-D3) method on the B3LYP-D3(BJ) theory level with 6-31G (d) in conjunction with the SMD continuum dielectric computations. As for these system with minor solvent (DCM), the solvent environment could be regarded as the same as the monomer (static dielectric constant of the IBVE, eps = 3.3). We constructed two anion-cation dimer models for each combination, with the anion positioned either above or below the cation. One configuration is more favorable for ion pair interactions, while the other is more conducive to forming hydrogen bonds. As for the IBVE cation and water, the latter configuration was selected.Then the intermolecular interaction energy of the optimized structures was calculated by DFT (B3LYP/6-311+G**). The

intermolecular interaction energy was calculated followed the equation $E_{int} = E_{dimer} - (E_{anion} + E_{cation})$.

## Supplementary Tables

**Table S1. Results of mechano-cRAFT polymerization of IBVE under various conditions**

| Entry[a] | Condition | Time (h) | Conversion[b] (%) |
|---|---|---|---|
| 1 | No $MoS_2$ | 2 | < 5 |
| 2 | No ball milling | 2 | < 5 |
| 3 | No TT-$CF_3^+$ $AsF_6^-$ | 2 | < 5 |
| 4 | 30 °C stirring | 2 | < 5 |
| 5 | LAG = 0.04 μL/mg | 2 | 71 |

[a]Reaction conditions: [IBVE] = 2.5 mmol, TT-$CF_3^+$ $AsF_6^-$ = 0.003 mmol, 1.6wt% loading $MoS_2$ (0.03 mmol). Ball mill (1.5 mL stainless-steel jar, 5 mm stainless-steel milling ball, 30 Hz), LAG ($\eta$ = 0.2 μL/mg) with DCM. Room temperature, under air. [b]Determined by $^1$H NMR in $CDCl_3$.

**Table S2. Results of water tolerance of $AsF_6^-$ initiated system under air.**

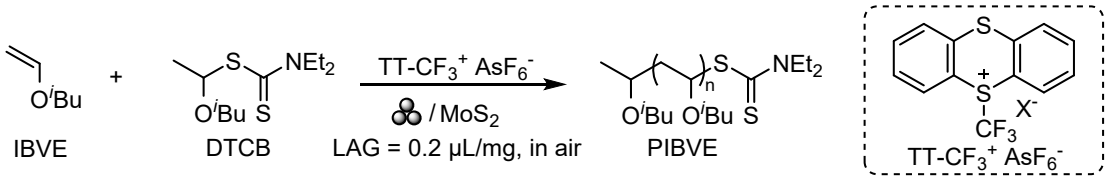


| Entry[a] | $H_2O$ (eq) | Time (h) | Conv. [%][b] | $M_{n,th}$ [kDa][c] | $M_{n,GPC}$ [kDa][d] | $Đ$[d] |
|---|---|---|---|---|---|---|
| 1 | 0 | 1.5 | 98 | 10.1 | 10.5 | 1.09 |
| 2 | 10 | 2 | 60 | 6.3 | 6.8 | 1.19 |

[a]Reaction conditions: [IBVE] = 2.5 mmol, TT-$CF_3^+$ $AsF_6^-$ = 0.003 mmol, 1.6wt% loading $MoS_2$ (0.03 mmol). Ball mill (1.5 mL stainless-steel jar, 5 mm stainless-steel milling ball, 30 Hz), LAG ($\eta$ = 0.2 μL/mg) with DCM. Room temperature, under air. [b]Determined by $^1$H NMR in $CDCl_3$. [c]$M_{n,th}$ = $[IBVE]_0/[DTCB]_0$ × conversion × $M_{IBVE}$ + $M_{DTCB}$. [d]Determined by GPC using polystyrene as calibration standard in THF.

**Table S3. Mechano-cRAFT polymerization of other vinyl ethers under Ar.**

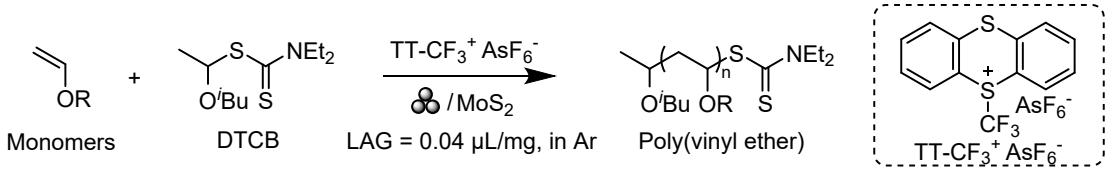


Monomers:

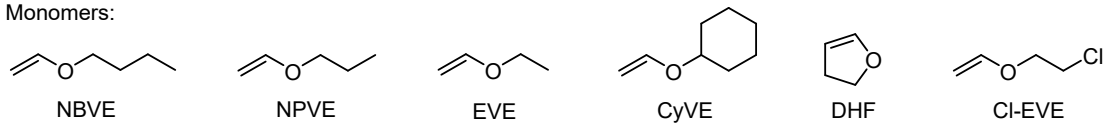

| Entry[a] | Monomer | $DP_T$ | Time (h) | Conv. [%][b] | $M_{n,th}$ [kDa][c] | $M_{n,GPC}$ [kDa][d] | $Đ$[d] |
|---|---|---|---|---|---|---|---|
| 1 | NBVE | 500 | 1.5 | 97 | 48.8 | 51.3 | 1.28 |
| 2 | | 1000 | 1.5 | 96 | 96.4 | 98.6 | 1.43 |
| 3 | NPVE | 500 | 1.5 | 99 | 42.9 | 44.1 | 1.25 |
| 4 | | 1000 | 1.5 | 99 | 85.5 | 88.9 | 1.40 |
| 5 | EVE | 500 | 1 | 99 | 35.9 | 37.6 | 1.24 |
| 6 | | 1000 | 1 | 99 | 71.6 | 63.9 | 1.44 |
| 7 | CyVE | 500 | 1 | 93 | 58.9 | 37.9 | 2.20 |
| 8 | | 1000 | 1 | 92 | 116.4 | 53.1 | 2.49 |
| 9[e] | | 1000 | 1 | 90 | 113.8 | 97.6 | 1.84 |
| 10 | DHF | 500 | 1 | 94 | 33.2 | 23.8 | 1.43 |
| 11 | | 1000 | 1 | 94 | 66.1 | 35.3 | 1.60 |
| 12[e] | | 1500 | 1 | 83 | 87.5 | 78.8 | 1.64 |
| 13 | Cl-EVE | 500 | 1.5 | 98 | 52.5 | 32.6 | 1.63 |
| 14 | | 1000 | 1.5 | 98 | 104.7 | 43.0 | 1.96 |

[a]Reaction conditions: [M] = 2.5 mmol, TT-$CF_3^+$ $AsF_6^-$ = 0.003 mmol, 0.7wt% loading $MoS_2$ (0.03 mmol). Ball mill (1.5 mL stainless-steel jar, 5 mm stainless-steel milling ball, 30 Hz), LAG ($\eta$ = 0.04 μL/mg) with DCM. Room temperature, under air. [b]Determined by $^1$H NMR in $CDCl_3$. [c]$M_{n,th} = [M]_0/[DTCB]_0 \times \text{conversion} \times M_M + M_{DTCB}$. [d]Determined by GPC using polystyrene as calibration standard in THF. [e] LAG = 0.2 μL/mg.

**Table S4. The simulation results of interaction energy between different counterions and IBVE dimer cation.**

| Dimer | TfO-IBVE | $BF_4$-IBVE | $AsF_6$-IBVE | $H_2O$-IBVE |
|---|---|---|---|---|
| Dimer 1 (hatree) | -1585.19 | -1048.15 | -3458.80 | -699.23 |
| Dimer 2 (hatree) | -1585.19 | -1048.14 | -3458.79 | / |
| cation (hatree) | -623.62 | -623.62 | -623.62 | -622.76 |
| anion (hatree) | -961.54 | -424.41 | -2835.04 | -76.47 |
| interaction 1 (hatree) | -0.034105 | -0.117229 | -0.141549 | -0.00461 |
| interaction 2 (hatree) | -0.034131 | -0.109053 | -0.134443 | / |
| interaction 1 (kcal/mol) | -21.40 | -73.56 | -88.82 | -2.90 |
| interaction 2 (kcal/mol) | -21.42 | -68.43 | -84.36 | / |

**Table S5. Summary of molecular weight of IBVE cationic polymerization in recent years.**

| Entry | $M_n$ (kDa) | $M_{n,th}$ (kDa) | $Đ$ | IBVE | Reference |
|---|---|---|---|---|---|
| 1[a] | 14.5 | 29.7 | 1.25 | undried | this work |
| 2[a] | 27.3 | 29.3 | 1.23 | undried | this work |
| 3[a] | 77.9 | 93.4 | 1.46 | undried | this work |
| 4[b] | 101 | 98.2 | 1.43 | undried | this work |
| 5[b] | 171.1 | 378.9 | 1.58 | undried | this work |
| 6[a] | 9.8 | 9.8 | 1.06 | dried | our previous work [1] |
| 7[a] | 26.4 | 59.4 | 1.26 | dried | our previous work [1] |
| 8 | 18.1 | 23 | 1.15 | undried | ref [4] |
| 9 | 65.7 | 57 | 1.14 | undried | ref [5] |
| 10 | 47.8 | 68.6 | 1.38 | undried | ref [6] |
| 11 | 40.6 | 39.9 | 1.19 | undried | ref [7] |
| 12 | 70.8 | 99.4 | 1.34 | undried | ref [7] |
| 13 | 25.7 | 40 | 1.21 | undried | ref [8] |
| 14 | 34 | 34 | 1.24 | undried | ref [9] |
| 15 | 80.1 | 100.1 | 1.37 | dried | ref [10] |
| 16 | 14.5 | 15.2 | 1.46 | dried | ref [11] |
| 17 | 160.4 | 200 | 1.68 | dried | ref [11] |
| 18 | 153 | 186.3 | 1.91 | dried | ref [12] |
| 19 | 35 | 40 | 1.3 | dried | ref [13] |
| 20 | 34.8 | 40 | 1.49 | dried | ref [14] |
| 21 | 22.5 | 28.8 | 1.33 | dried | ref [15] |
| 22 | 32.6 | 34.6 | 1.45 | dried | ref [16] |
| 23 | 65.3 | 80.5 | 1.24 | dried | ref [17] |
| 24 | 104 | 104 | 1.23 | dried | ref [18] |
| 25 | 22.5 | 20.2 | 1.19 | dried | ref [19] |
| 26 | 25.4 | 30.3 | 1.48 | dried | ref [20] |
| 27 | 19.2 | 20.3 | 1.54 | dried | ref [21] |
| 28 | 37.1 | 40.2 | 1.18 | dried | ref [22] |
| 29 | 55 | 50 | 1.14 | dried | ref [23] |

[a]Reaction in air. [b]Reaction in Ar.

## Supplementary Figures

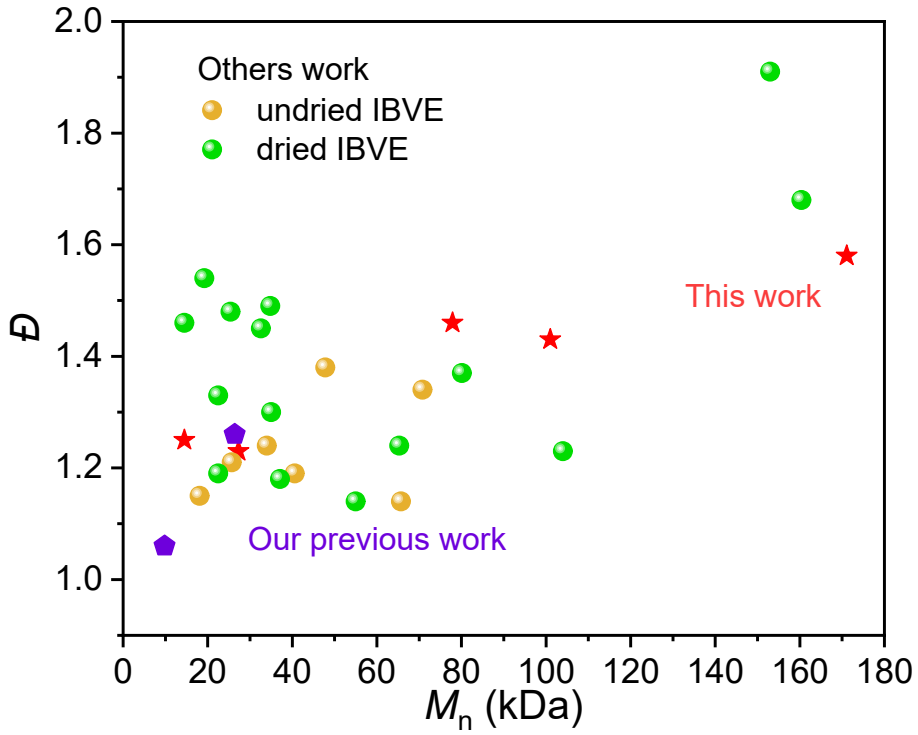


**Figure S1.** Scatter plot for comparing the molecular weight of IBVE cationic polymerization in recent years (date from Table S5).

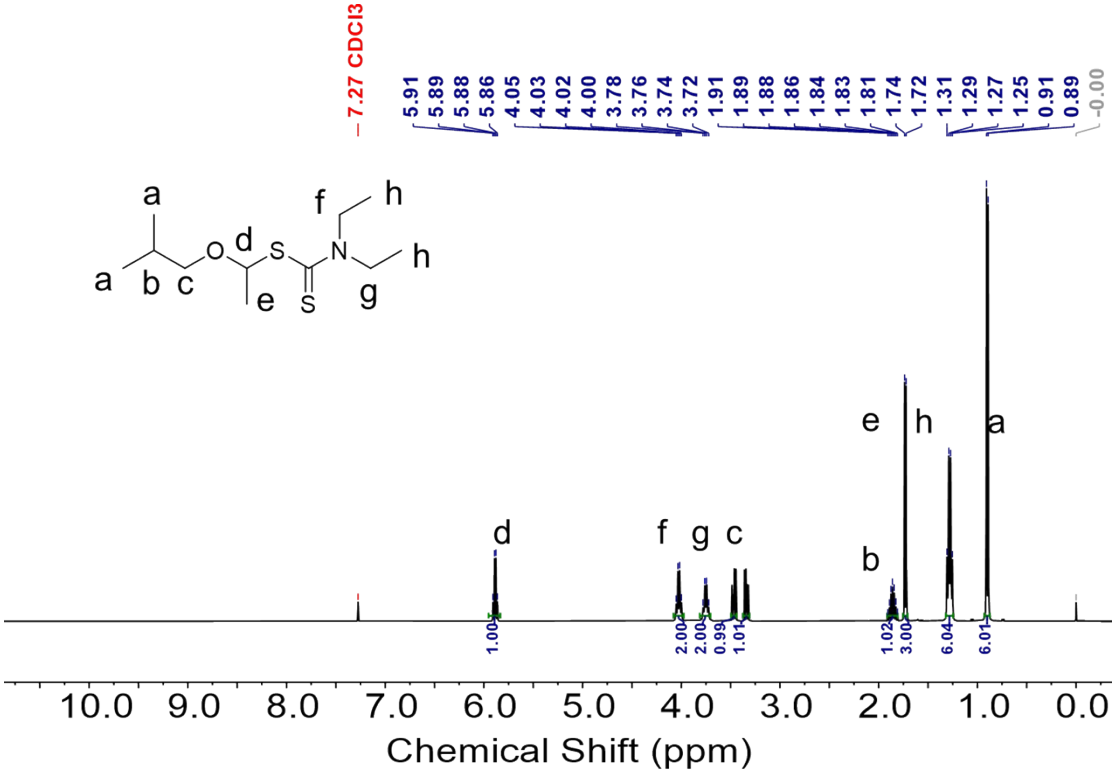


**Figure S2.** $^1$H NMR spectrum of *S*-1-isobutoxyethyl *N, N*-diethyl dithiocarbamate (DTCB) in $CDCl_3$.

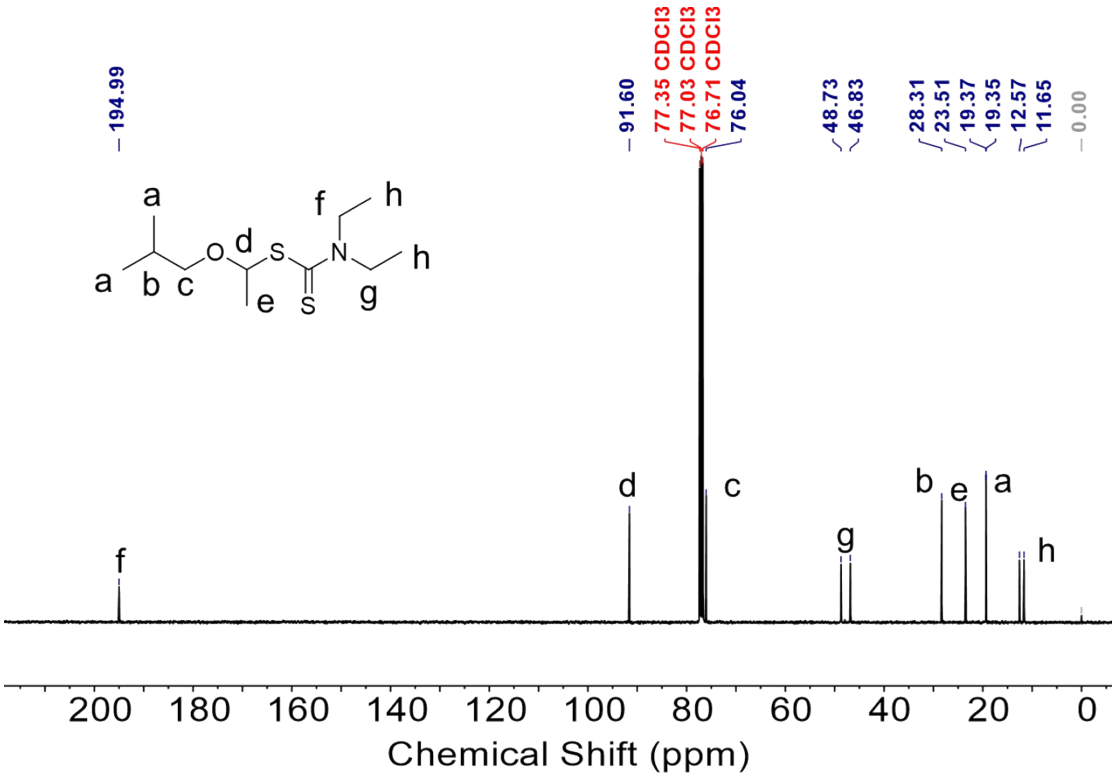


**Figure S3.** $^{13}C$ NMR spectrum of *S*-1-isobutoxyethyl *N, N*-diethyl dithiocarbamate (DTCB) in $CDCl_3$.

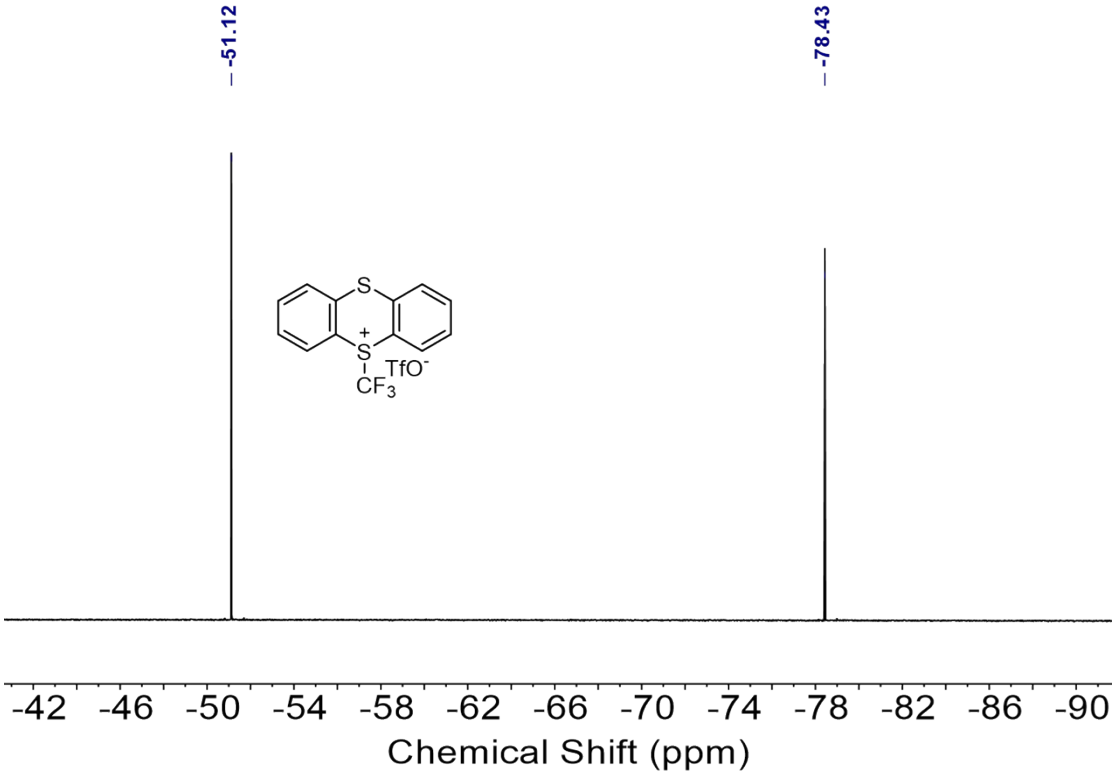


**Figure S4.** $^{19}F$ NMR spectrum of initiator **c** (TT-$CF_3^+$ $TfO^-$) in acetone-d6.

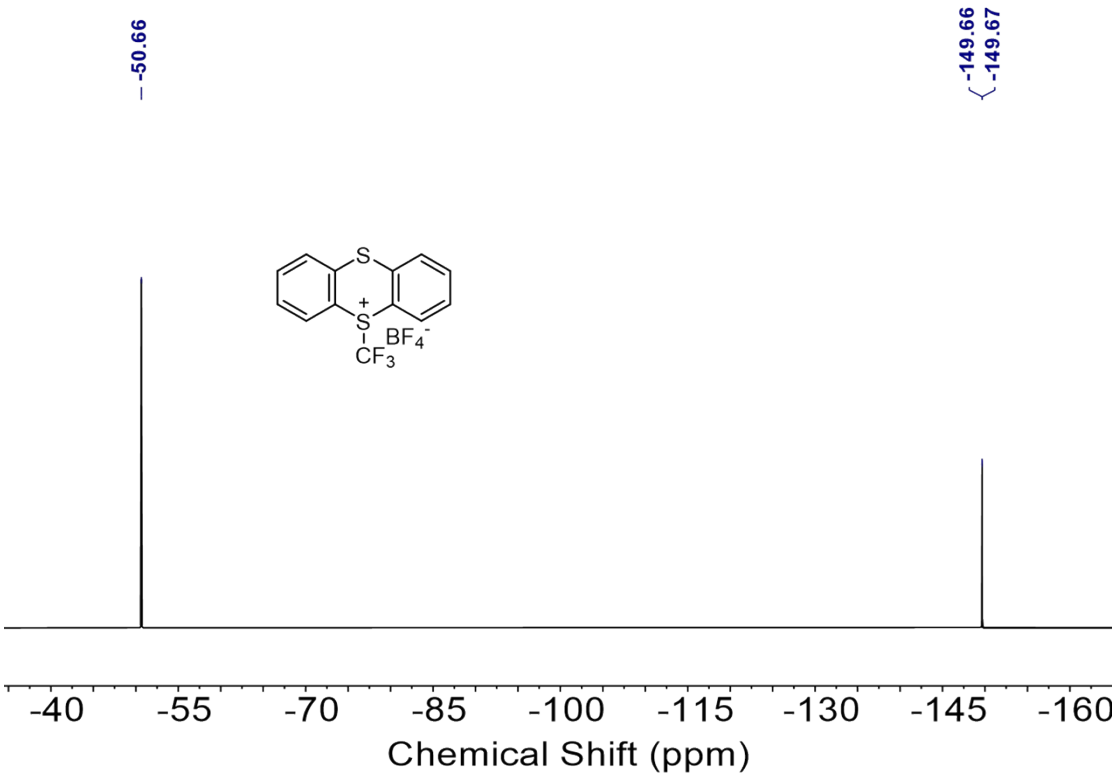


**Figure S5.** $^{19}F$ NMR spectrum of initiator **d** (TT-$CF_3^+$ $BF_4^-$) in acetone-d6.

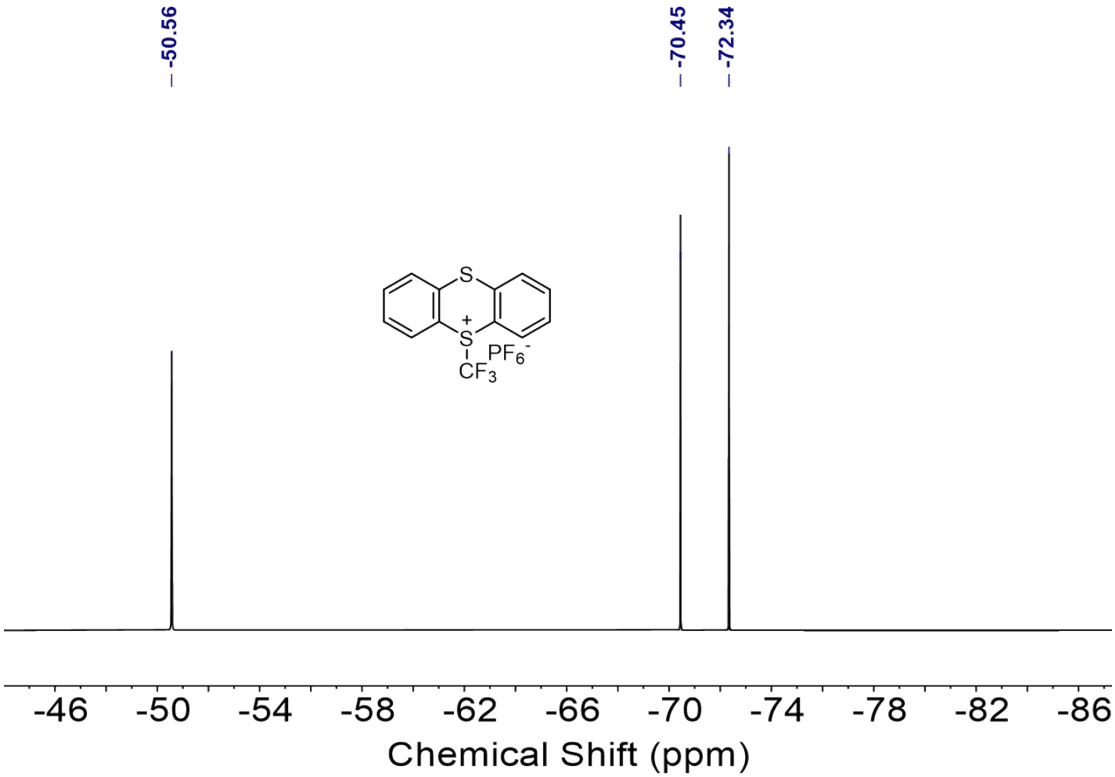


**Figure S6.** $^{19}F$ NMR spectrum of initiator **e** (TT-$CF_3^+$ $PF_6^-$) in acetone-d6.

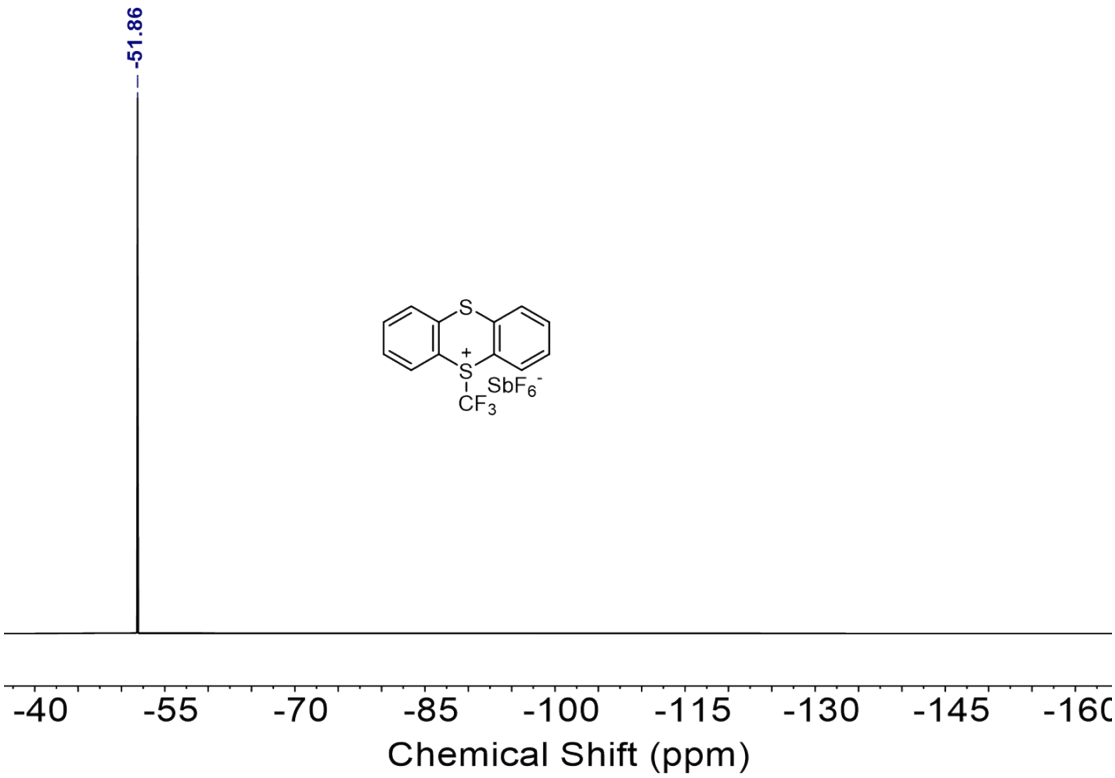


**Figure S7.** $^{19}F$ NMR spectrum of initiator **f** (TT-$CF_3^+$ $SbF_6^-$) in acetone-d6.

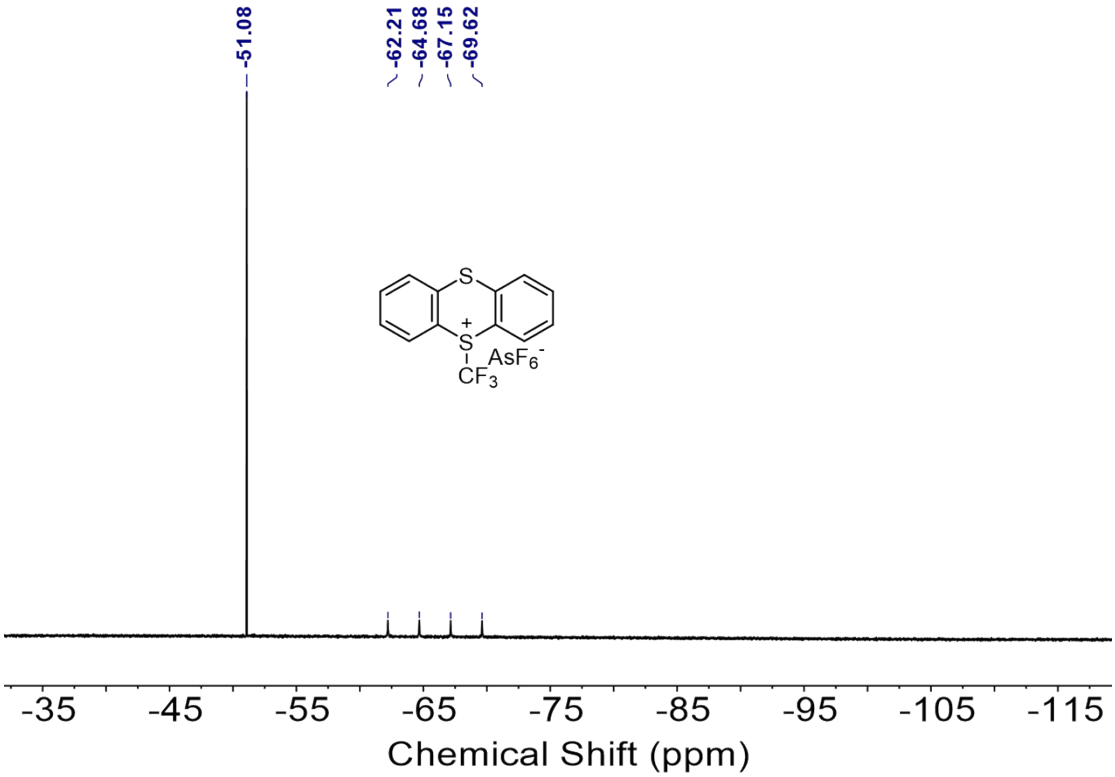


**Figure S8.** $^{19}F$ NMR spectrum of initiator **g** (TT-$CF_3^+$ $AsF_6^-$) in acetone-d6.

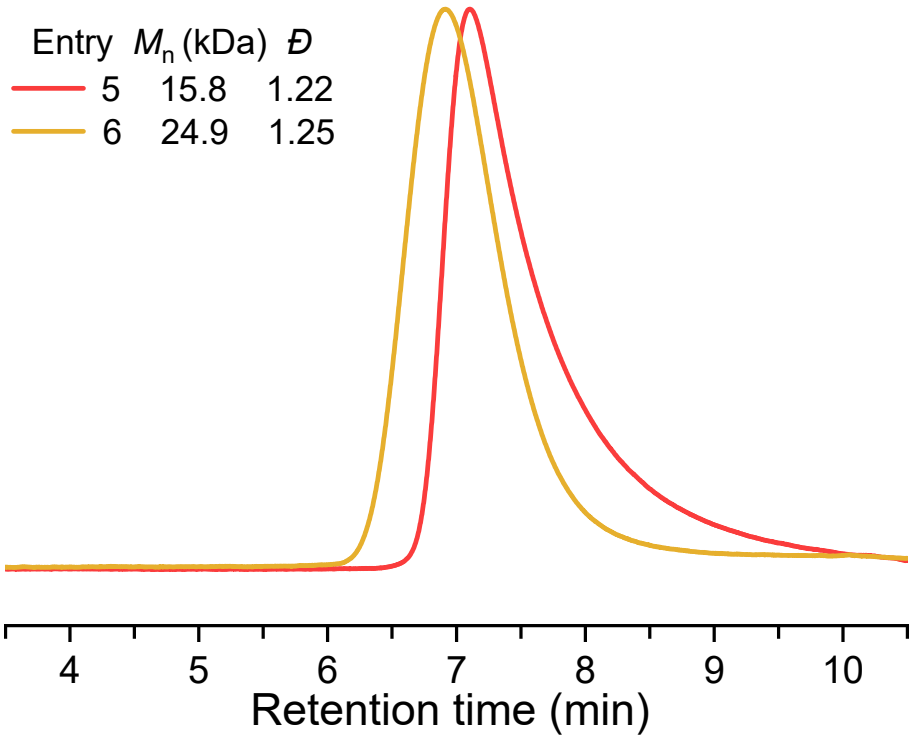


**Figure S9.** GPC traces of PIBVE with different counterions under air (Table 1, entries 5-6).

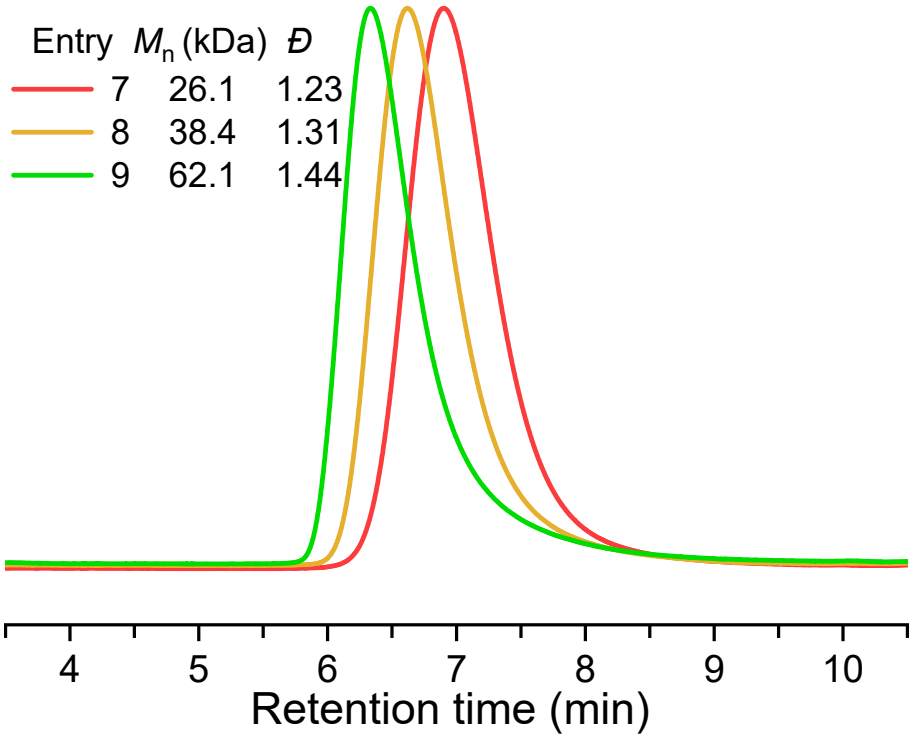


**Figure S10.** GPC traces of PIBVE using **e** (TT-$CF_3^+PF_6^-$) as initiator under air (Table 1, entries 7-9).

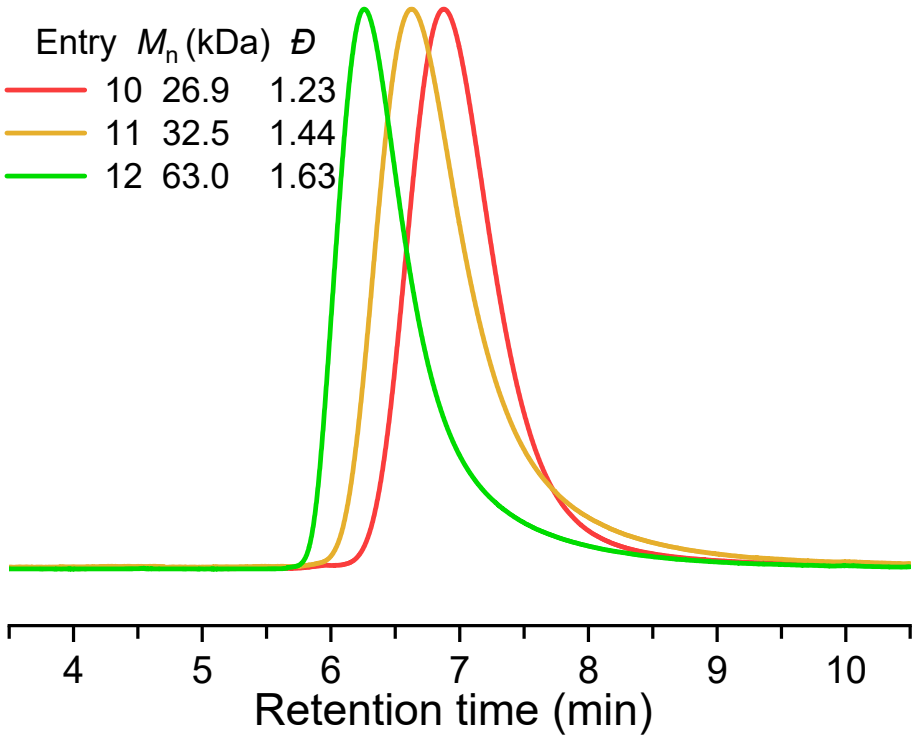


**Figure S11.** GPC traces of PIBVE using **f** (TT-$CF_3^+$ $SbF_6^-$) as initiator under air (Table 1, entries 10-12).

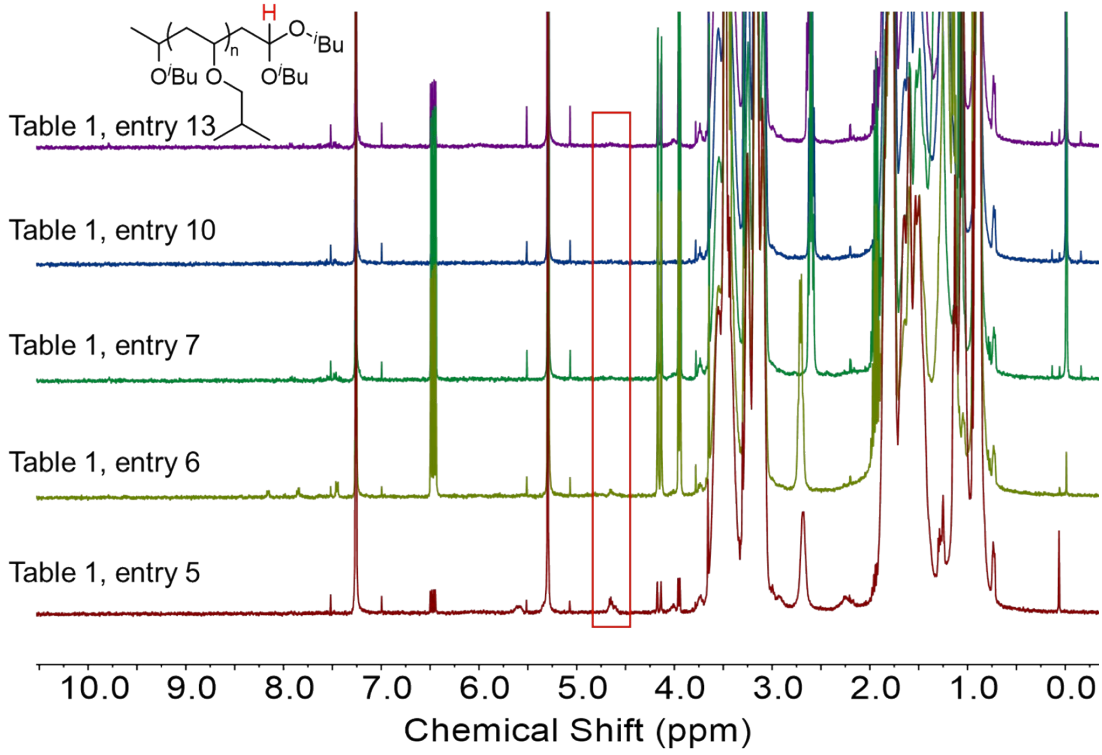


**Figure S12.** $^1$H NMR spectra of mechano-cRAFT polymerization mixture of IBVE with different TT-type initiators.

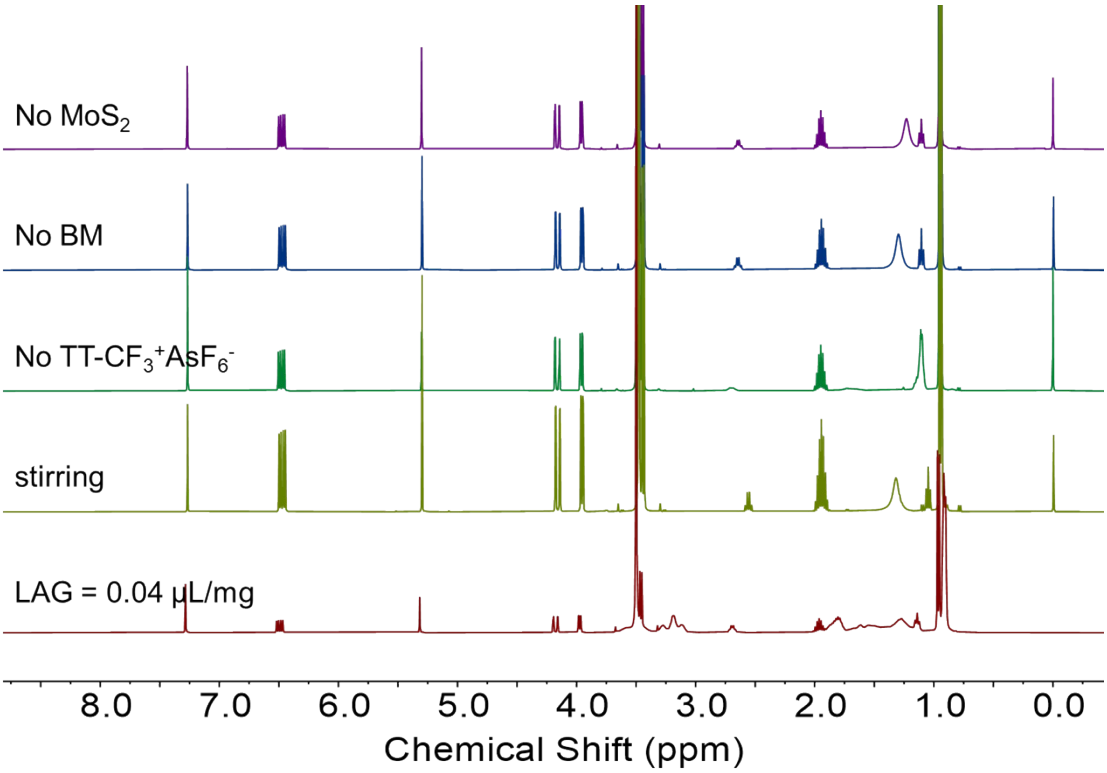


**Figure S13.** $^1$H NMR spectra of mechano-cRAFT polymerization mixture of IBVE with different control experiments (Table S1).

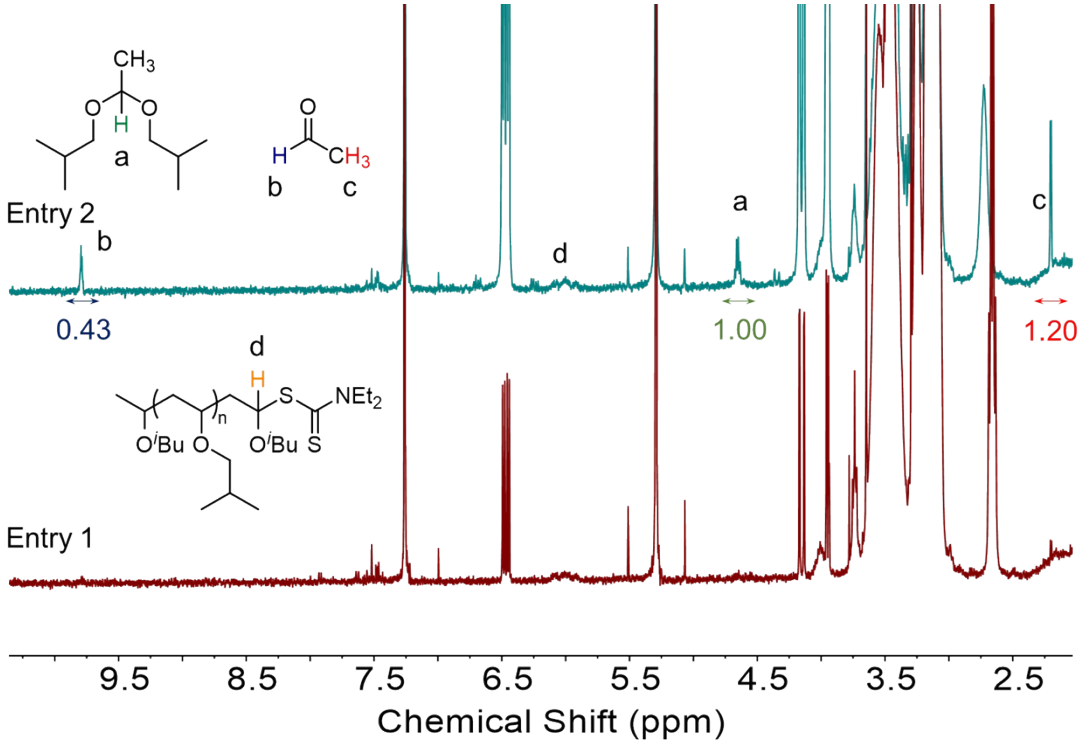


**Figure S14.** $^1$H NMR spectra of polymerization mixture of IBVE using **g** (TT-$CF_3^+$ $AsF_6^-$) as initiator under the condition of adding 10 equivalents of water (Table S2).

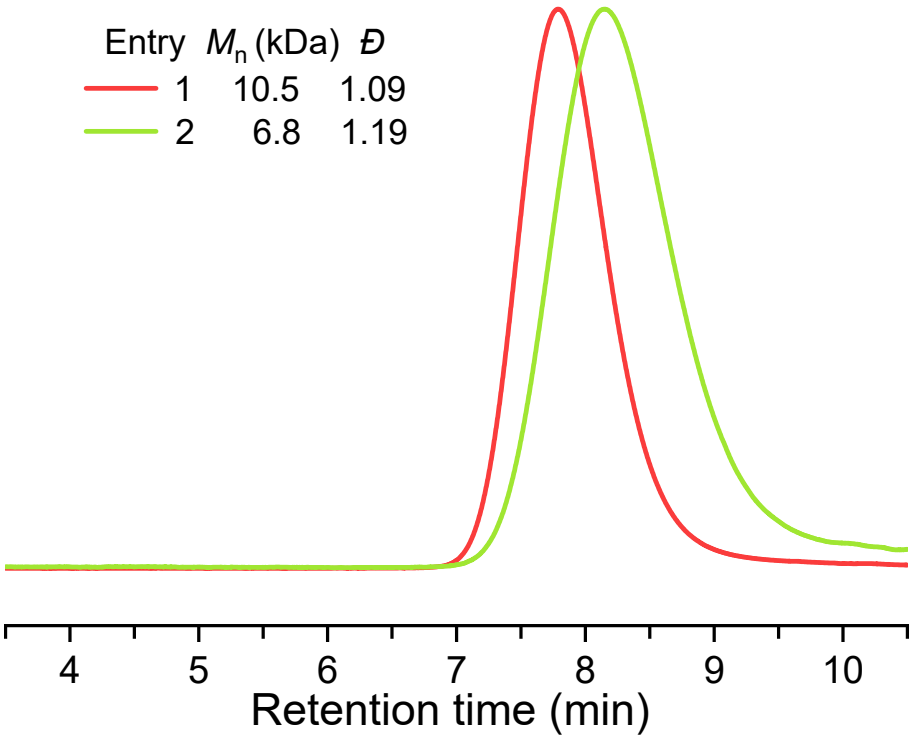


**Figure S15.** GPC traces of PIBVE using **g** (TT-$CF_3^+$ $AsF_6^-$) as initiator under the condition of adding 10 equivalents of water (Table S2, entries 1-2).

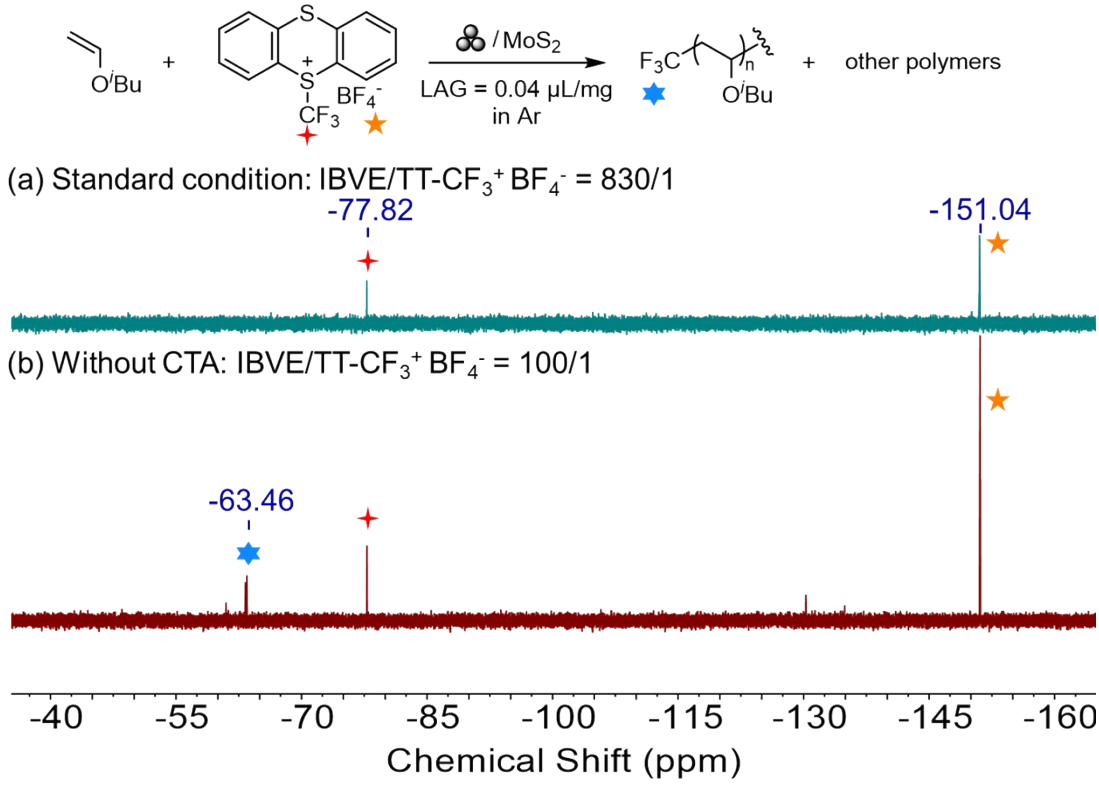


**Figure S16.** $^{19}F$ NMR spectra of PIBVE with different polymerization conditions. (a) Cationic RAFT polymerization. (b) Cationic polymerization.

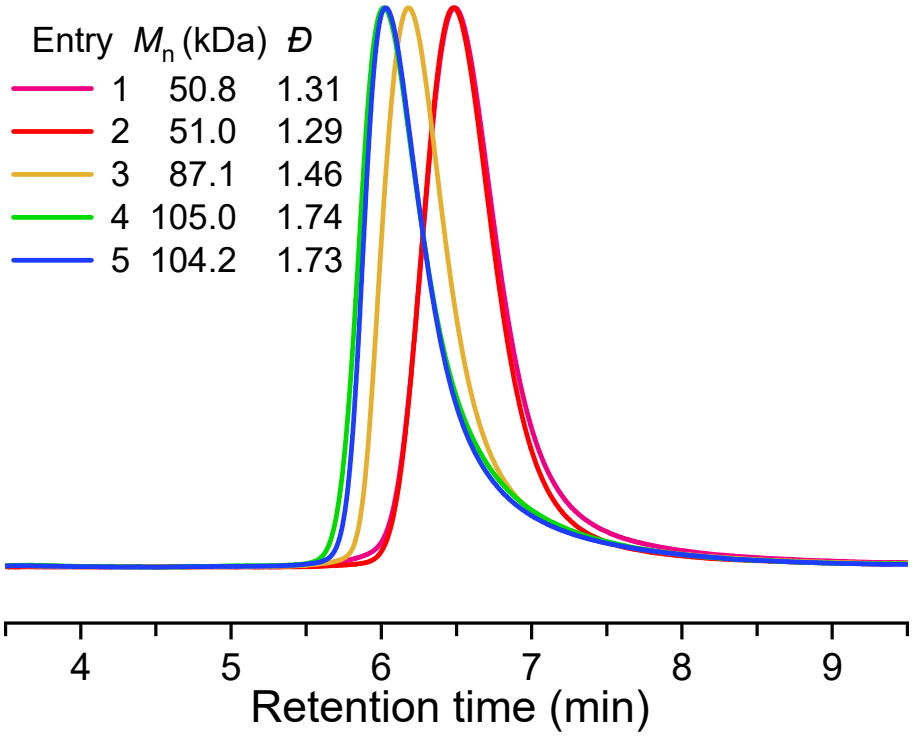


**Figure S17.** GPC traces of PIBVE using **d** (TT-$CF_3^+$ $BF_4^-$) as initiator under Ar (Table 2, entries 1-5).

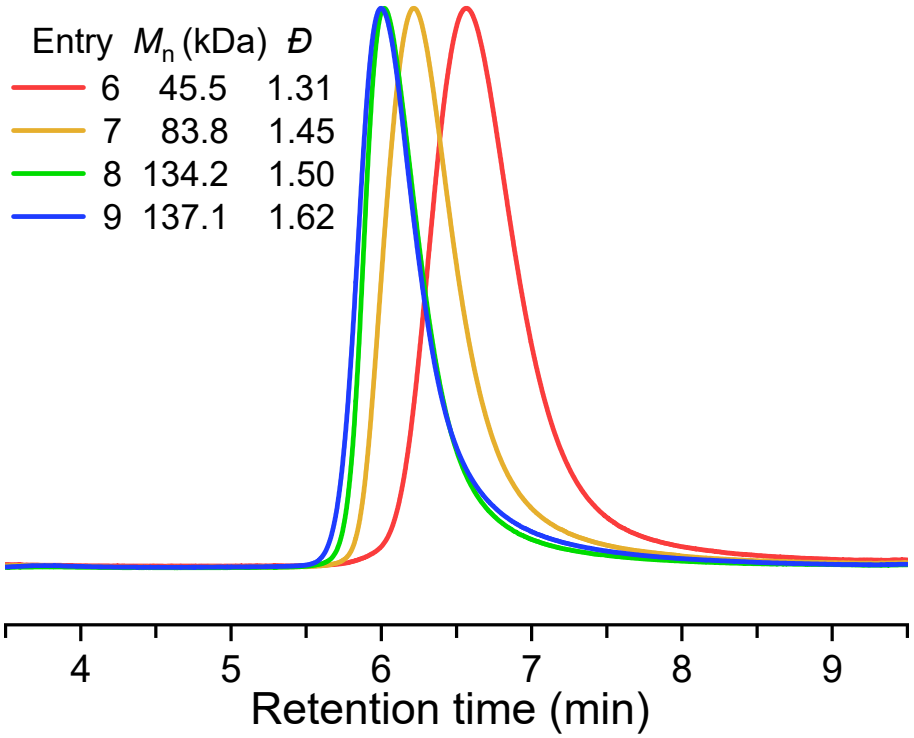


**Figure S18.** GPC traces of PIBVE using **e** (TT-$CF_3^+$ $PF_6^-$) as initiator under Ar (Table 2, entries 6-9).

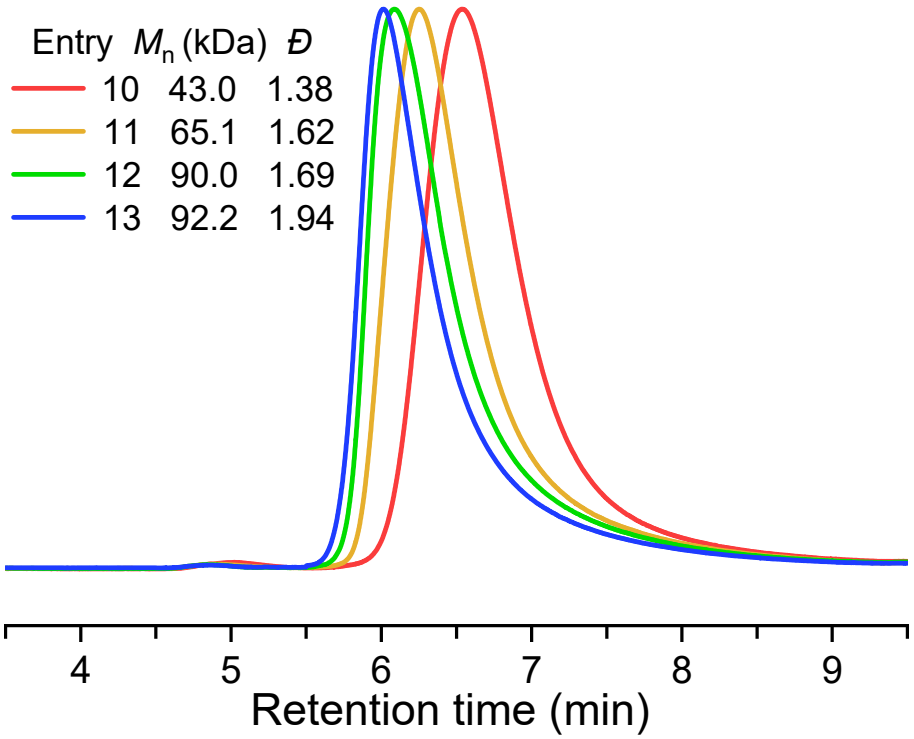


**Figure S19.** GPC traces of PIBVE using **f** (TT-$CF_3^+$ $SbF_6^-$) as initiator under Ar (Table 2, entries 10-13).

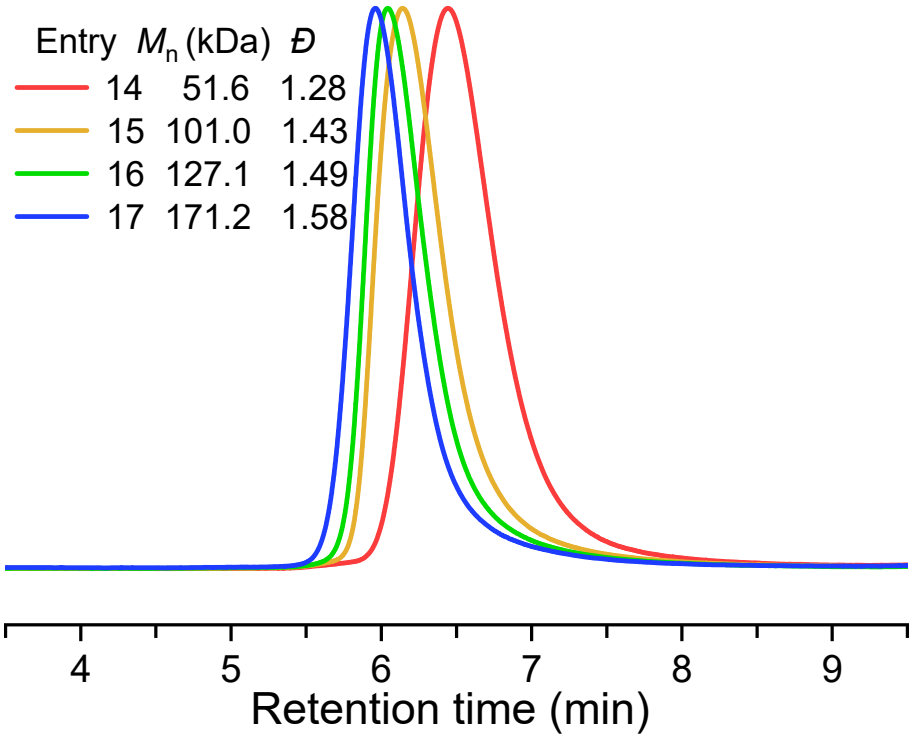


**Figure S20.** GPC traces of PIBVE using **g** (TT-$CF_3^+$ $AsF_6^-$) as initiator under Ar (Table 2, entries 14-17).

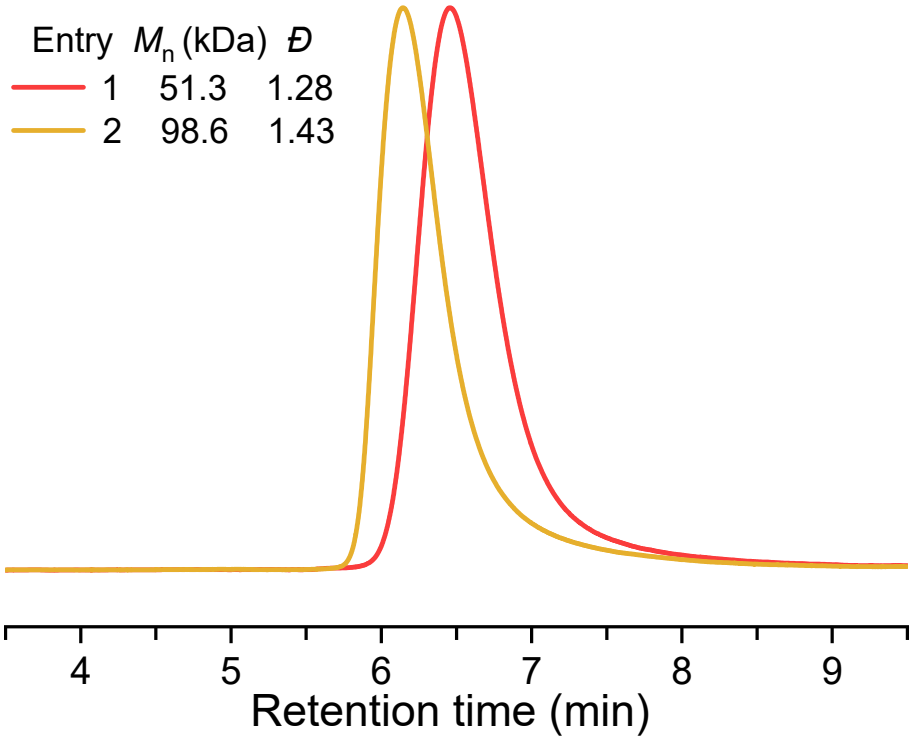


**Figure S21.** GPC traces of PNBVE with different $DP_T$ (Table S3, entries 1-2).

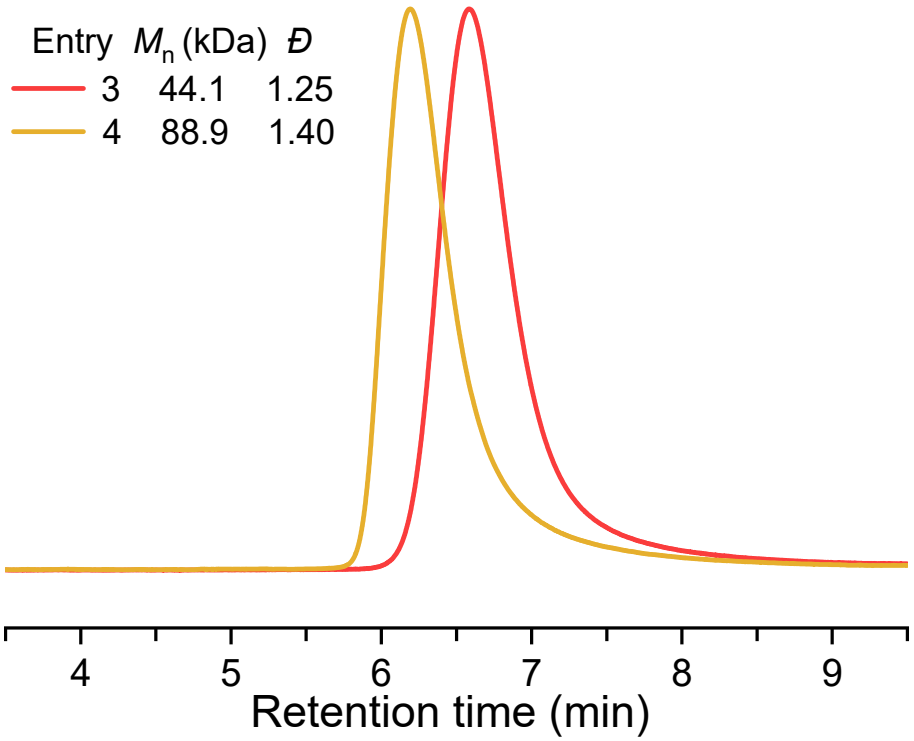


**Figure S22.** GPC traces of PNPVE with different $DP_T$ (Table S3, entries 3-4).

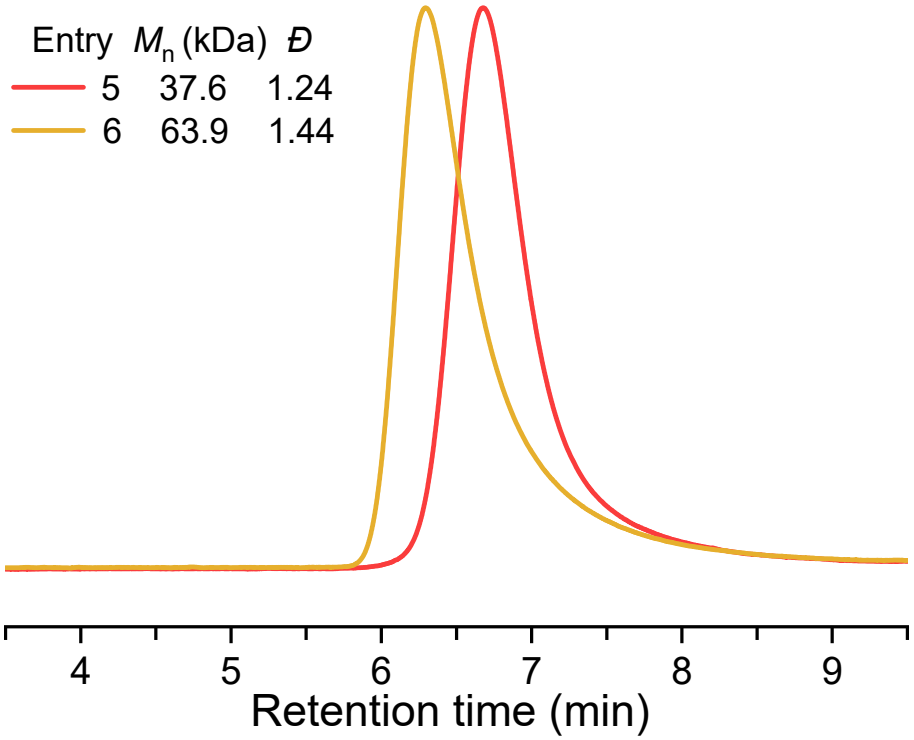


**Figure S23.** GPC traces of PEVE with different $DP_T$ (Table S3, entries 5-6).

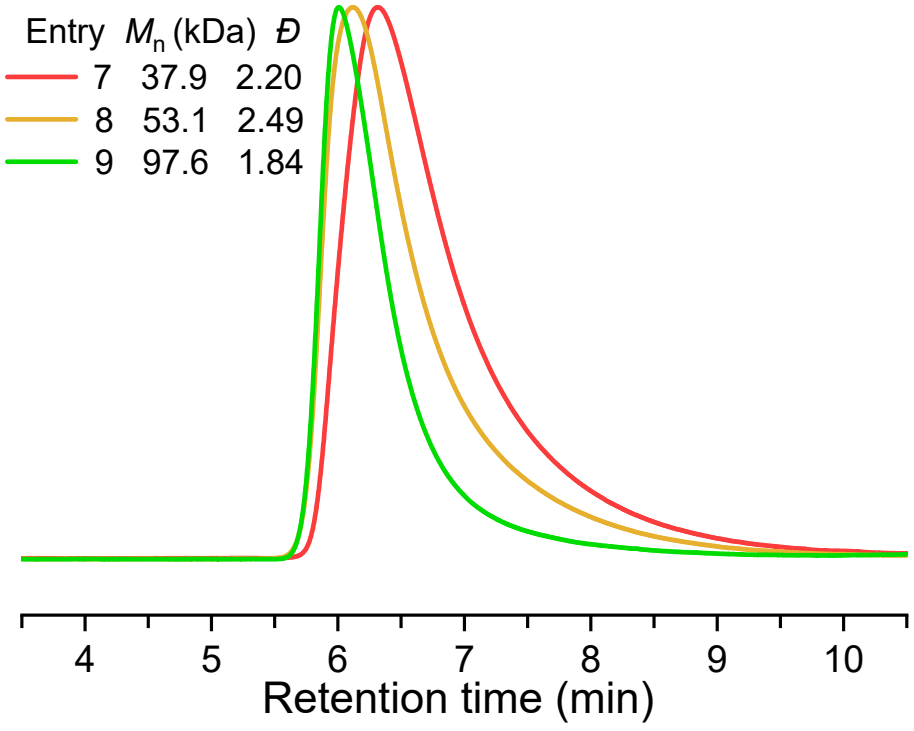


**Figure S24.** GPC traces of PCyVE with different $DP_T$ (Table S3, entries 7-9).

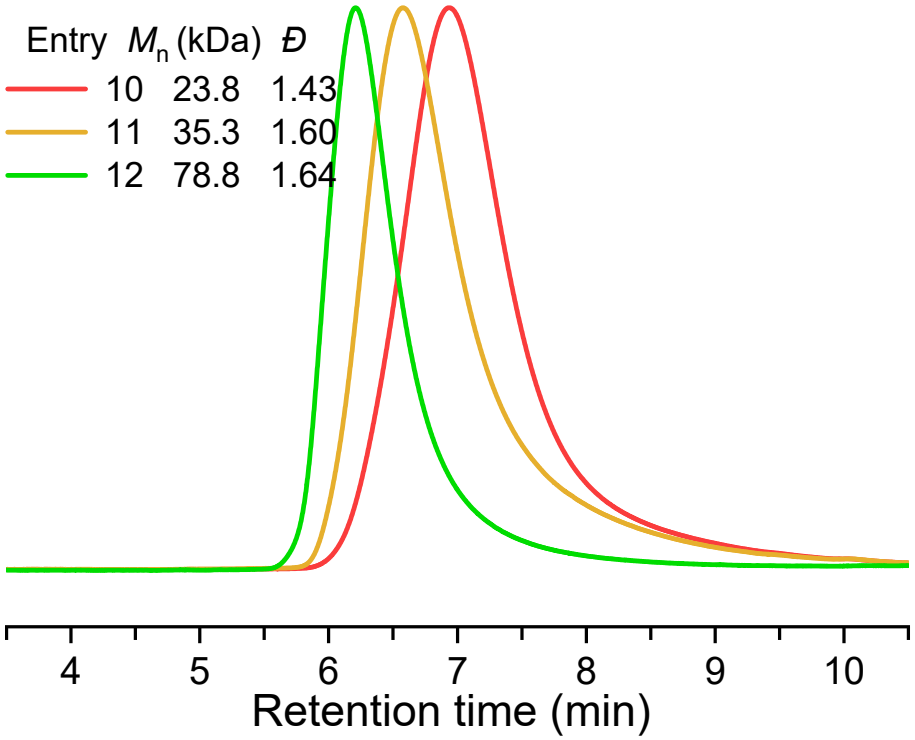


**Figure S25.** GPC traces of PDHF with different $DP_T$ (Table S3, entries 10-12).

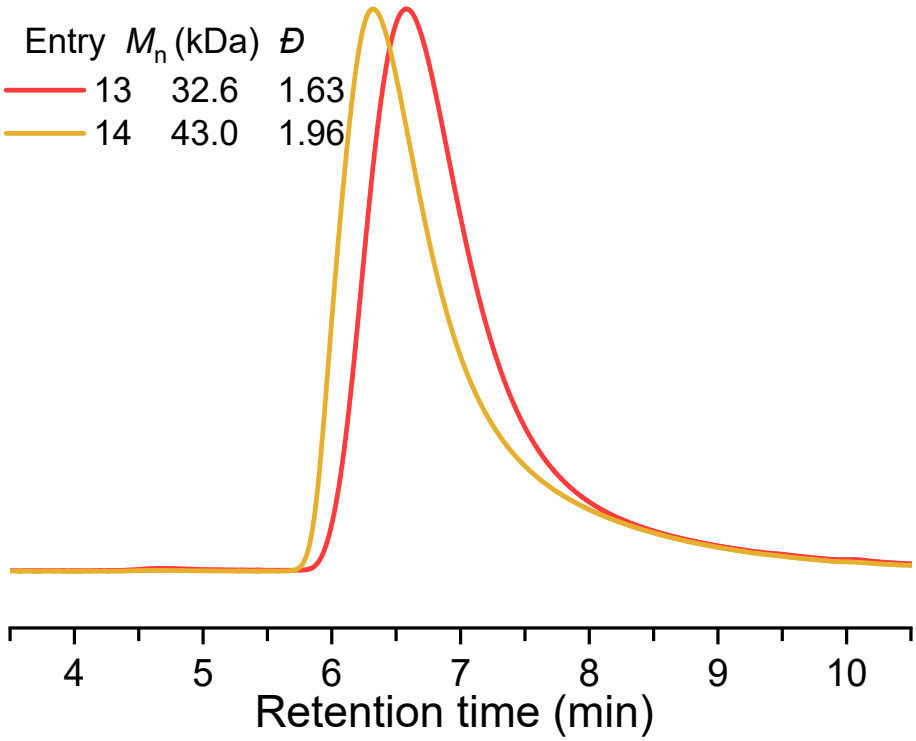


**Figure S26.** GPC traces of P(Cl-EVE) with different $DP_T$ (Table S3, entries 13-14).

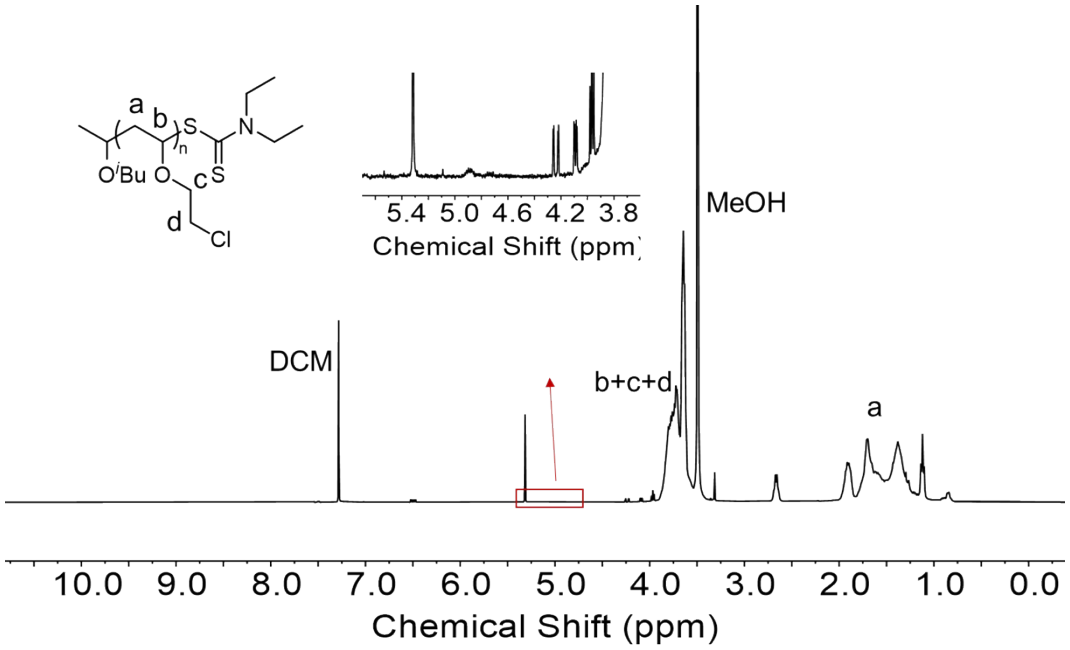


**Figure S27.** $^1$H NMR spectrum of polymerization mixture of Cl-EVE (Table S3, entry 13).

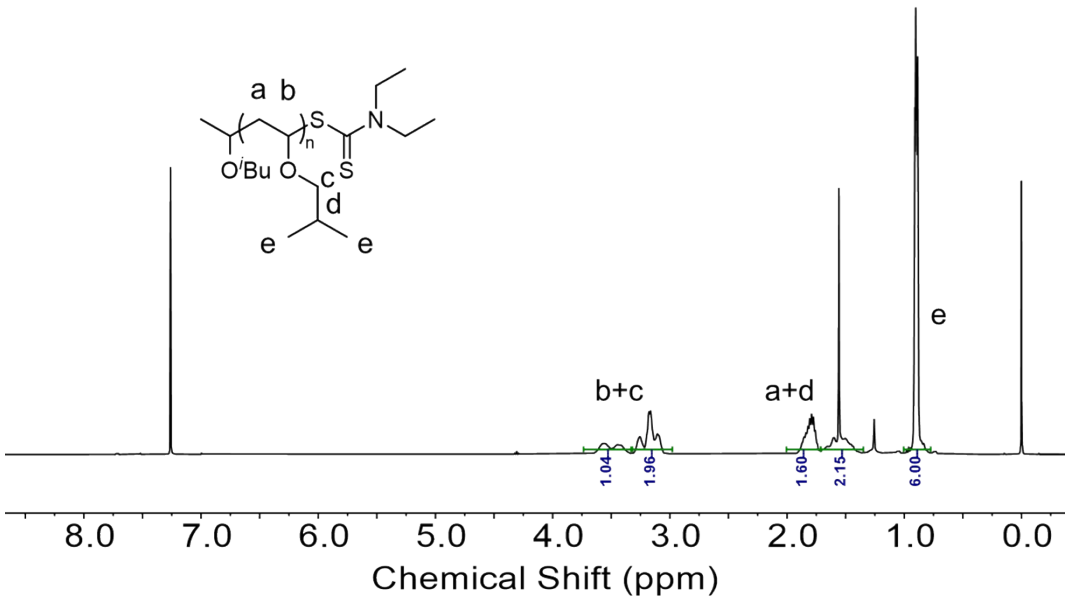


**Figure S28.** $^1$H NMR spectrum of P(IBVE) in $CDCl_3$ ($M_n$ = 51.6 kDa).

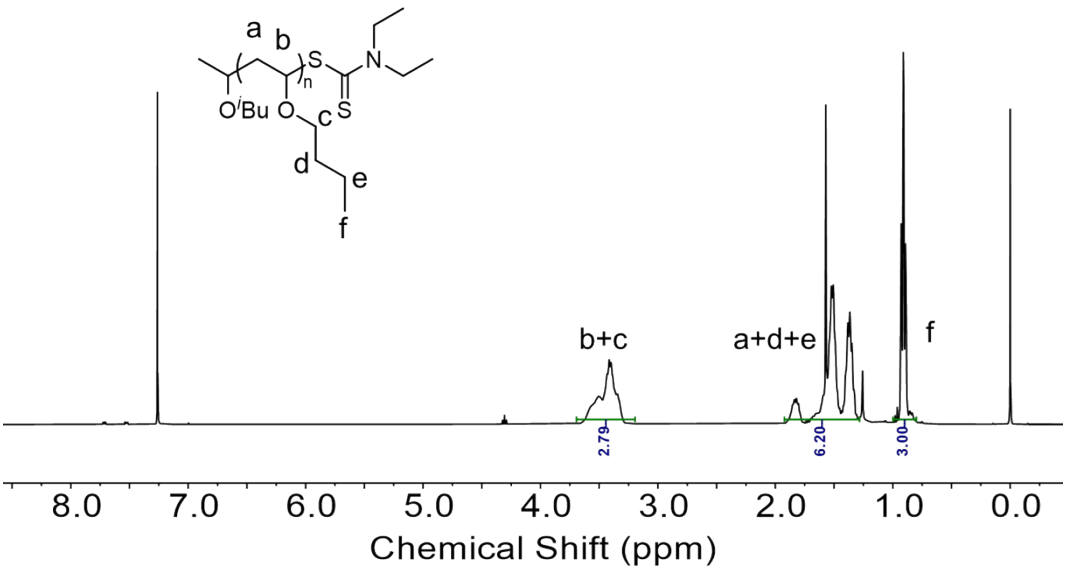


**Figure S29.** $^{1}$H NMR spectrum of P(NBVE) in $CDCl_3$ ($M_n$ = 51.3 kDa).

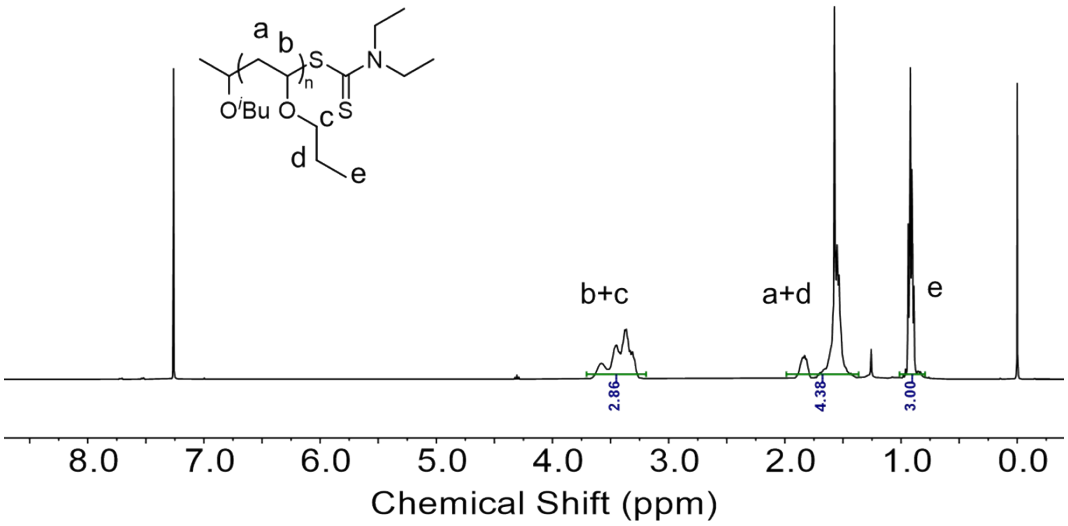


**Figure S30.** $^{1}$H NMR spectrum of P(NPVE) in $CDCl_3$ ($M_n$ = 44.1 kDa).

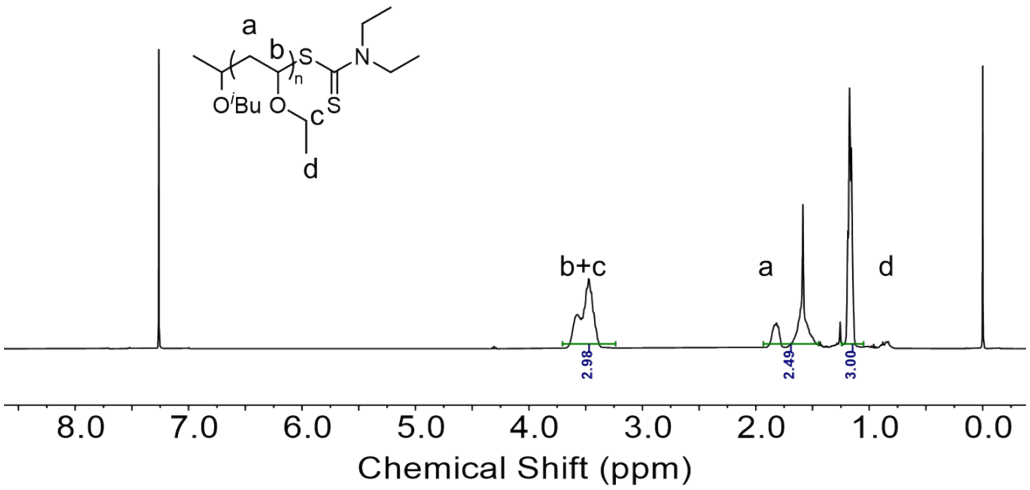


**Figure S31.** $^1$H NMR spectrum of P(EVE) in $CDCl_3$ ($M_n$ = 37.6 kDa).

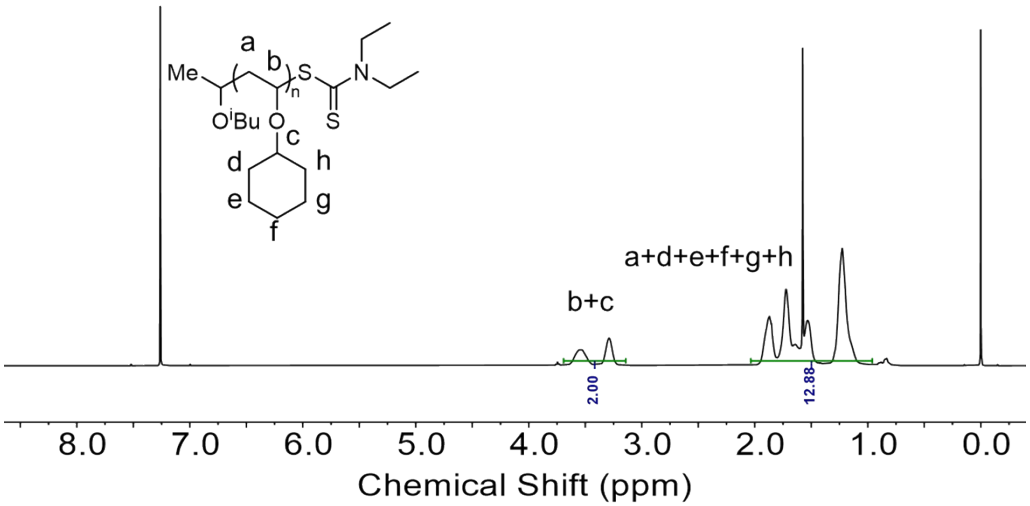


**Figure S32.** $^1$H NMR spectrum of P(CyVE) in $CDCl_3$ ($M_n$ = 37.9 kDa).

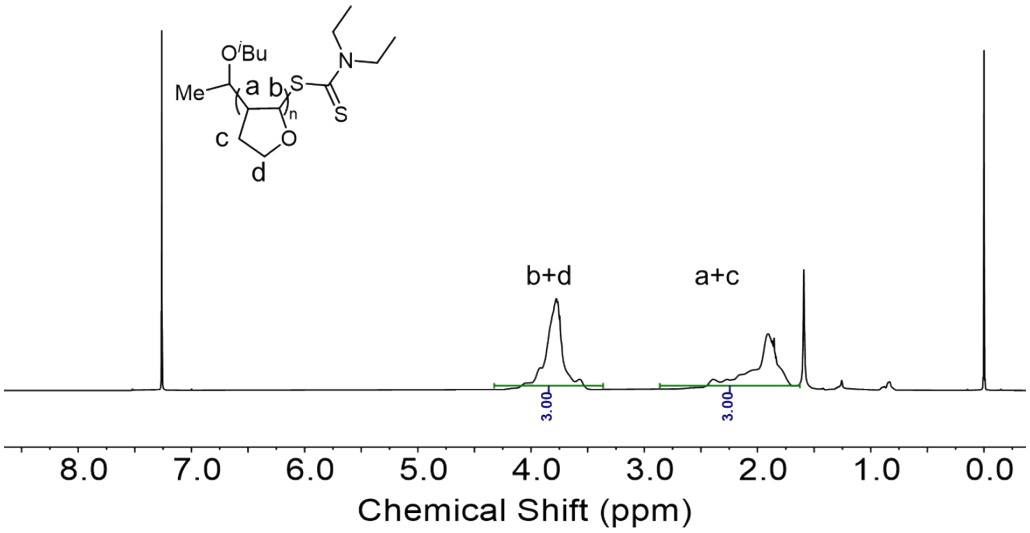


**Figure S33.** $^1$H NMR spectrum of PDHF in $CDCl_3$ ($M_n$ = 23.8 kDa).

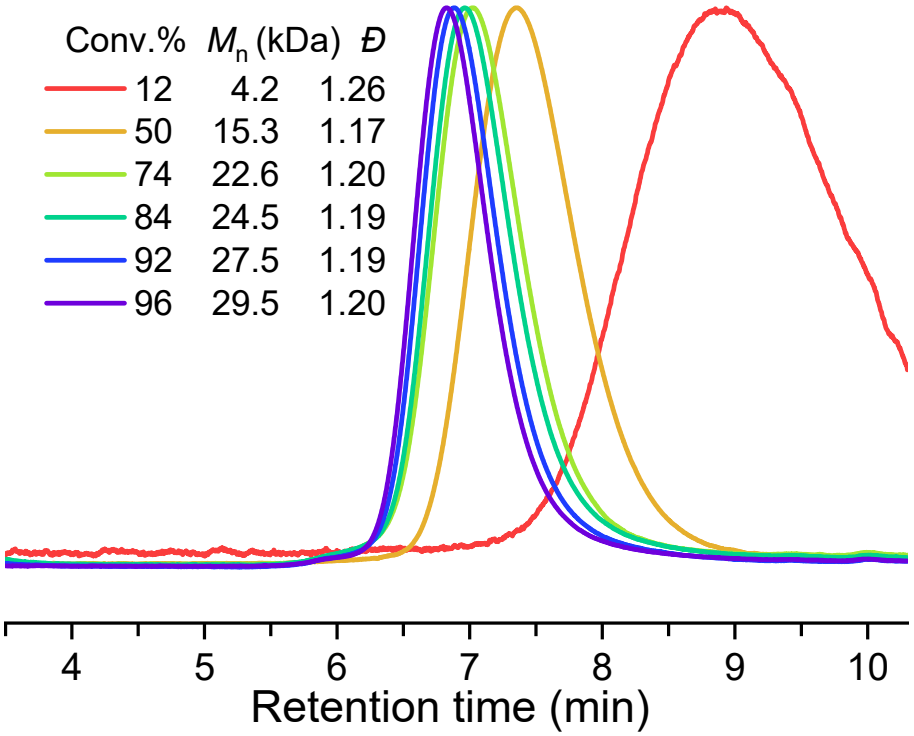


**Figure S34.** GPC traces of PIBVE at different conversions in polymerization kinetics using **d** (TT-$CF_3^+$ $BF_4^-$) as initiator.

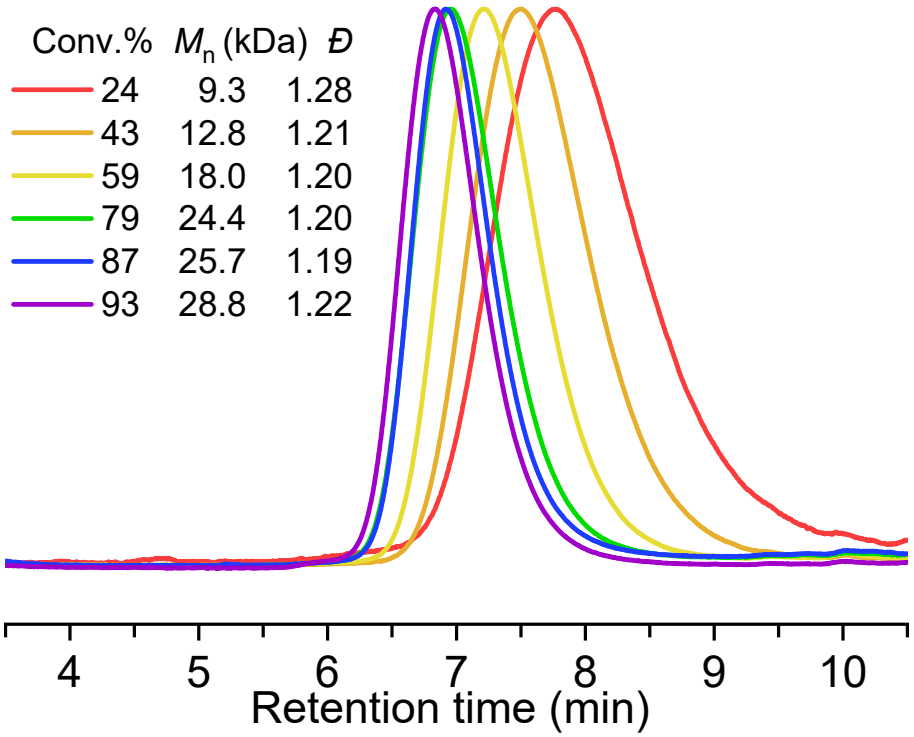


**Figure S35.** GPC traces of PIBVE at different conversions in polymerization kinetics using **e** (TT-$CF_3^+$ $PF_6^-$) as initiator.

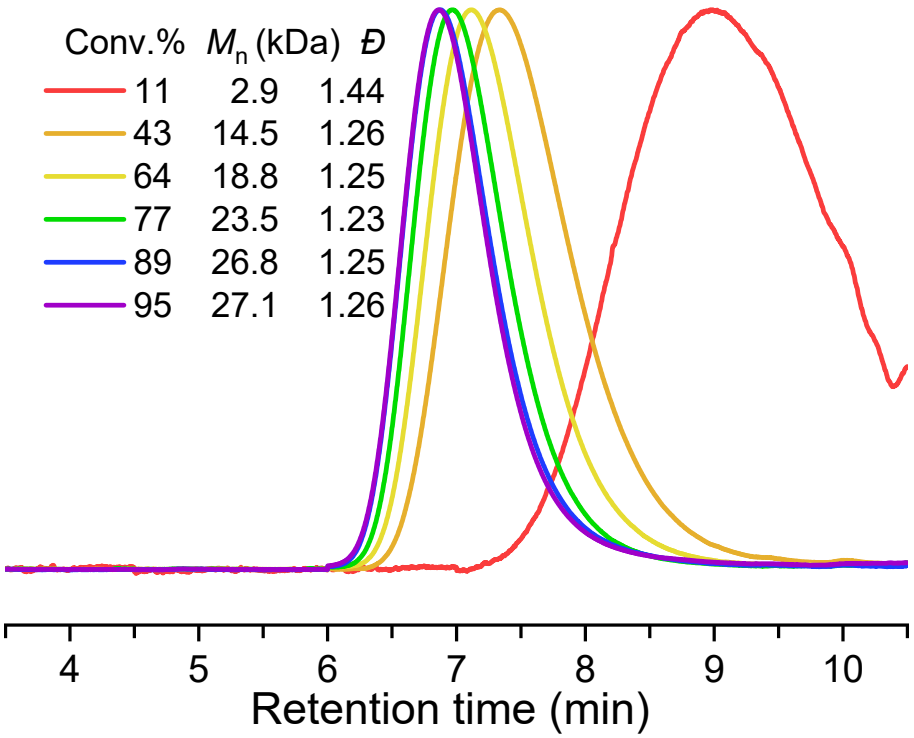


**Figure S36.** GPC traces of PIBVE at different conversions in polymerization kinetics using **f** (TT-$CF_3^+$ $SbF_6^-$) as initiator.

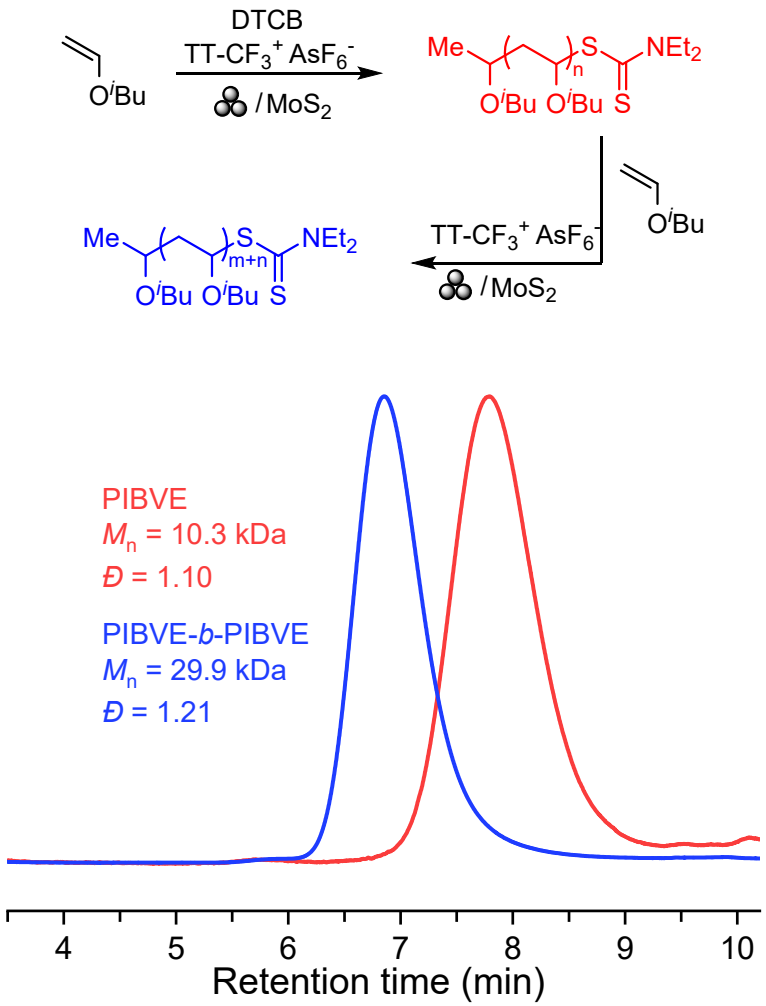


**Figure S37.** GPC traces for PIBVE-*b*-PIBVE ($DP_{T,\ IBVE1}$ = 100, $DP_{T,\ IBVE2}$ = 200).

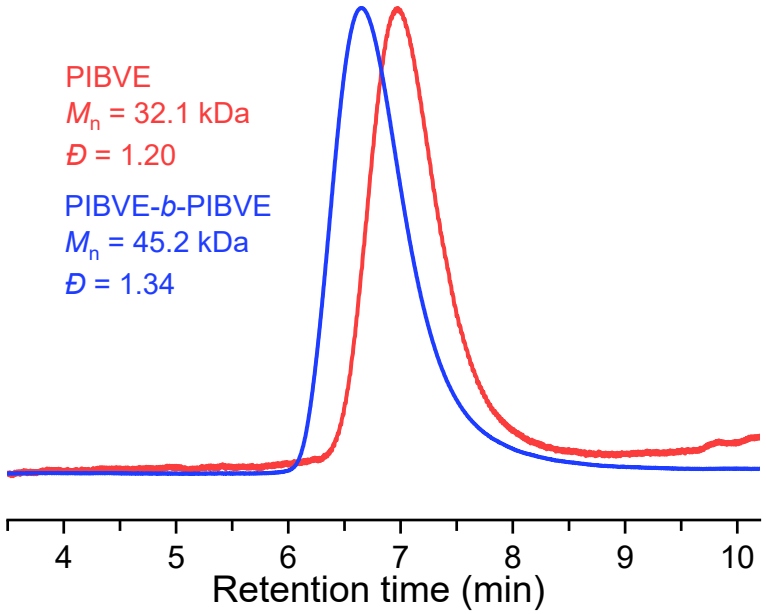


**Figure S38.** GPC traces for PIBVE-*b*-PIBVE ($DP_{T,\ IBVE1}$ = 300, $DP_{T,\ IBVE2}$ = 300).

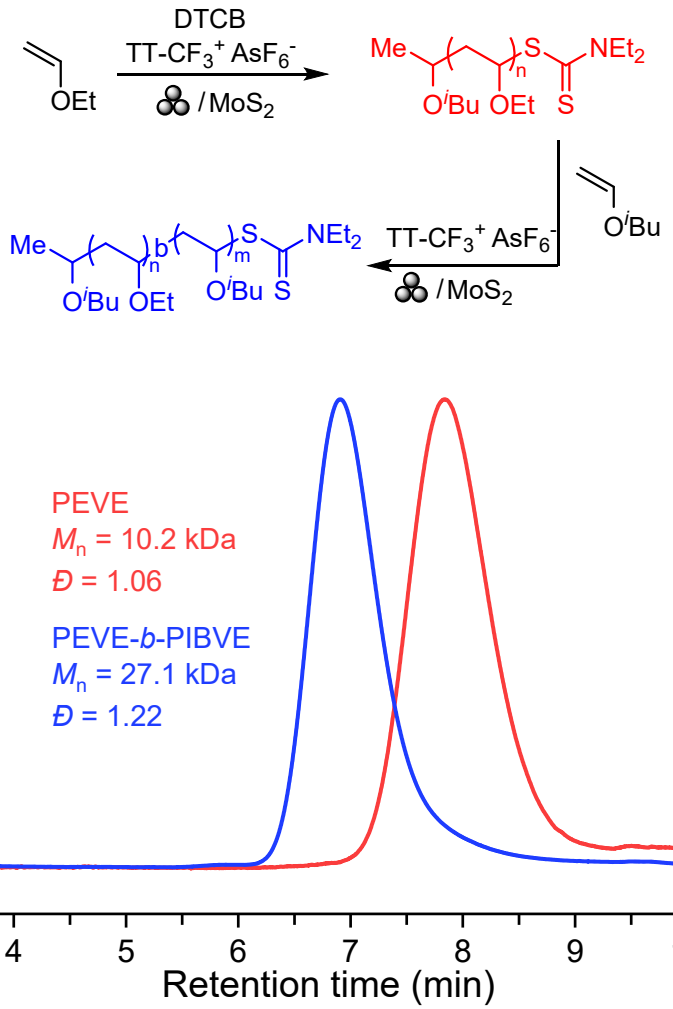


**Figure S39.** GPC traces for PEVE-*b*-PIBVE ($DP_{T,\,EVE1}$ = 140, $DP_{T,\,IBVE2}$ = 200).

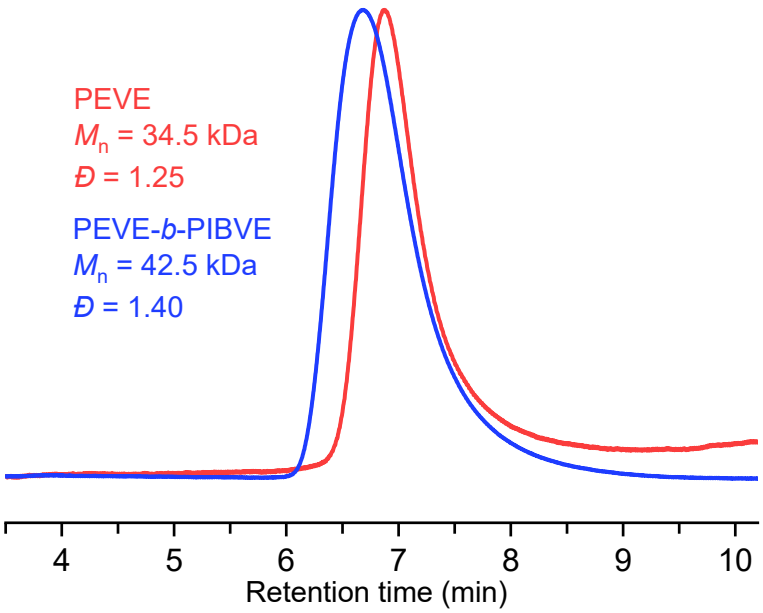


**Figure S40.** GPC traces for PEVE-*b*-PIBVE ($DP_{T,\,EVE1}$ = 420, $DP_{T,\,IBVE2}$ = 300).

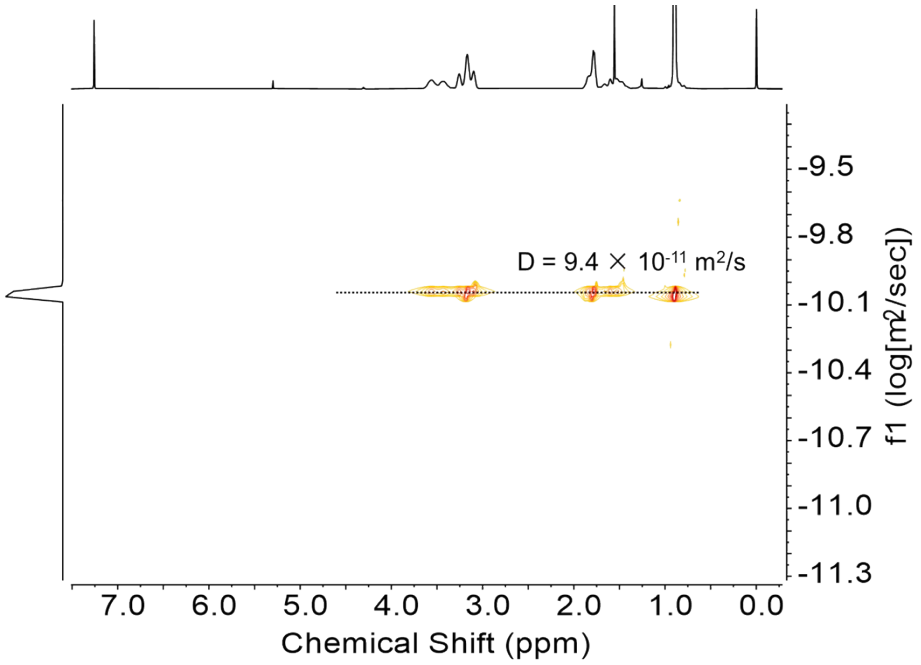


**Figure S41.** $^{1}$H DOSY spectrum of PIBVE-*b*-PIBVE ($M_n$ = 29.3 kDa; Figure 3e).

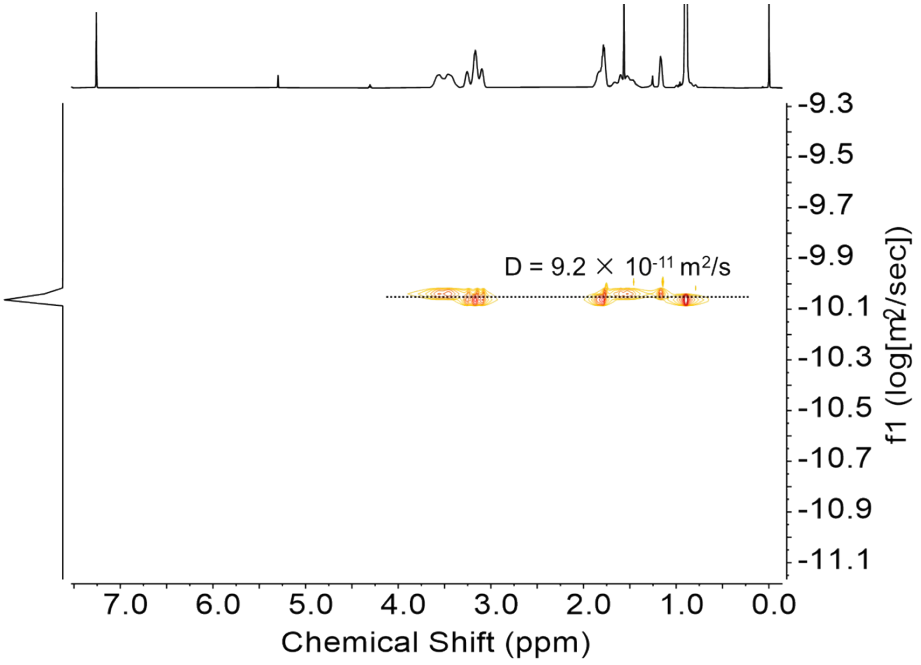


**Figure S42.** $^{1}$H DOSY spectrum of PEVE-*b*-PIBVE ($M_n$ = 29.6 kDa; Figure 3f).

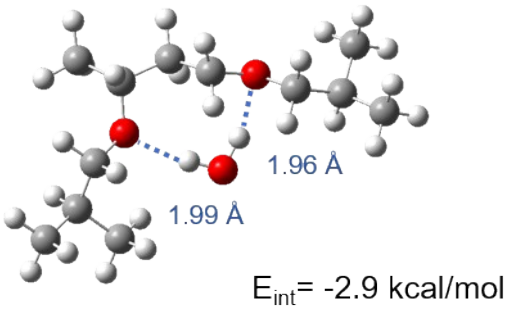


**Figure S43.** DFT calculation of the interaction between water and oxocarbenium ion. (Noting: The computational method, SMD solvation model, and all other parameters were kept consistent to ensure comparison at the same theoretical level. The calculated interaction energies may contain deviations due to factors such as the choice of DFT functional, basis set, initial molecular conformation, and the specific solvation environment applied in the SMD model.)

## Reference

(1) Zhang, L.; Zou, X.; Ding, C.; Wang, Z. Mechanically induced cationic reversible addition–fragmentation chain transfer polymerization of vinyl ethers. *Chem. Sci.* **2024**, *15* (45), 18977-18984.
(2) Zhao, B.; Li, J.; Li, Z.; Lin, X.; Pan, X.; Zhang, Z.; Zhu, J. Photoinduced 3D Printing through a Combination of Cationic and Radical RAFT Polymerization. *Macromolecules* **2022**, *55* (16), 7181-7192.
(3) Jia, H.; Häring, A. P.; Berger, F.; Zhang, L.; Ritter, T. Trifluoromethyl Thianthrenium Triflate: A Readily Available Trifluoromethylating Reagent with Formal $CF_3^+$, $CF_3^{\bullet}$, and $CF_3^-$ Reactivity. *J. Am. Chem. Soc.* **2021**, *143* (20), 7623-7628.
(4) Kottisch, V.; O'Leary, J.; Michaudel, Q.; Stache, E. E.; Lambert, T. H.; Fors, B. P. Controlled Cationic Polymerization: Single-Component Initiation under Ambient Conditions. *J. Am. Chem. Soc.* **2019**, *141* (27), 10605-10609.
(5) Kottisch, V.; Jermaks, J.; Mak, J. Y.; Woltornist, R. A.; Lambert, T. H.; Fors, B. P. Hydrogen Bond Donor Catalyzed Cationic Polymerization of Vinyl Ethers. *Angew. Chem. Int. Edit.* **2020**, *60* (9), 4535-4539.
(6) Shankel, S. L.; Lambert, T. H.; Fors, B. P. Moisture tolerant cationic RAFT polymerization of vinyl ethers. *Polym. Chem.* **2022**, *13* (42), 5974-5979.
(7) Lin, X.; Li, J.; Zhang, J.; Liu, S.; Lin, X.; Pan, X.; Zhu, J.; Zhu, X. Living cationic polymerization of vinyl ethers initiated by electrophilic selenium reagents under ambient conditions. *Polym. Chem.* **2021**, *12* (7), 983-990.
(8) Zhang, M.; Li, J.; Chen, M.; Pan, X.; Zhang, Z.; Zhu, J. Combination of the Photoinduced Atom Transfer Radical Addition Reaction and Living Cationic Polymerization: A Latent Initiator Strategy toward Tailoring Polymer Molecular Weight Distributions. *Macromolecules* **2021**, *54* (13), 6502-6510.
(9) Li, J.; Kerr, A.; Song, Q.; Yang, J.; Häkkinen, S.; Pan, X.; Zhang, Z.; Zhu, J.; Perrier, S. Manganese-Catalyzed Batch and Continuous Flow Cationic RAFT Polymerization Induced by Visible Light. *ACS Macro Lett.* **2021**, *10* (5), 570-575.
(10) Lin, X.; Gu, Q.; Li, J.; Zhu, J. Zinc-Mediated Living Cationic Polymerization. *ACS Macro Lett.* **2023**, 1692-1697.
(11) Zhang, X.; Yang, Z.; Jiang, Y.; Liao, S. Organocatalytic, Stereoselective, Cationic Reversible Addition–Fragmentation Chain-Transfer Polymerization of Vinyl Ethers. *J. Am. Chem. Soc.* **2022**, *144* (2), 679-684.
(12) Ciftci, M.; Yoshikawa, Y.; Yagci, Y. Living Cationic Polymerization of Vinyl Ethers through a Photoinduced Radical Oxidation/Addition/Deactivation Sequence. *Angew. Chem. Int. Edit.* **2017**, *56* (2), 519-523.
(13) Kottisch, V.; Michaudel, Q.; Fors, B. P. Cationic Polymerization of Vinyl Ethers Controlled by Visible Light. *J. Am. Chem. Soc.* **2016**, *138* (48), 15535-15538.
(14) Sifri, R. J.; Kennedy, A. J.; Fors, B. P. Photocontrolled cationic degenerate chain transfer polymerizations via thioacetal initiators. *Polym. Chem.* **2020**, *11* (40), 6499-6504.
(15) Peterson, B. M.; Lin, S.; Fors, B. P. Electrochemically Controlled Cationic

Polymerization of Vinyl Ethers. *J. Am. Chem. Soc.* **2018**, *140* (6), 2076-2079.
(16) Kottisch, V.; Supej, M. J.; Fors, B. P. Enhancing Temporal Control and Enabling Chain-End Modification in Photoregulated Cationic Polymerizations by Using Iridium-Based Catalysts. *Angew. Chem. Int. Edit.* **2018**, *57* (27), 8260-8264.
(17) Peterson, B. M.; Kottisch, V.; Supej, M. J.; Fors, B. P. On Demand Switching of Polymerization Mechanism and Monomer Selectivity with Orthogonal Stimuli. *ACS Cent. Sci.* **2018**, *4* (9), 1228-1234.
(18) Uchiyama, M.; Satoh, K.; Kamigaito, M. Cationic RAFT Polymerization Using ppm Concentrations of Organic Acid. *Angew. Chem. Int. Edit.* **2015**, *54* (6), 1924-1928.
(19) Zhang, L.; Jiang, K.; Shen, X.; Gu, Y.; Lin, X.; Chen, M. Thienyl Chloride Initiated Living Cationic Polymerization: A General and Efficient Access toward Terminally Functionalized Poly(vinyl ether)s. *Macromolecules* **2020**, *53* (5), 1536-1542.
(20) Zhang, X.; Jiang, Y.; Ma, Q.; Hu, S.; Liao, S. Metal-Free Cationic Polymerization of Vinyl Ethers with Strict Temporal Control by Employing an Organophotocatalyst. *J. Am. Chem. Soc.* **2021**, *143* (17), 6357-6362.
(21) Yang, Z.; Liao, Y.; Zhang, Z.; Chen, J.; Zhang, X.; Liao, S. Asymmetric Ion-Pairing Photoredox Catalysis for Stereoselective Cationic Polymerization under Light Control. *J. Am. Chem. Soc.* **2024**, *146* (10), 6449-6455.
(22) Li, M.; Zhang, Z.; Yan, Y.; Lv, W.; Li, Z.; Wang, X.; Tao, Y. Anion-binding catalysis enables living cationic polymerization. *Nat. Synth.* **2022**, *1* (10), 815-823.
(23) Sang, W.; Yan, Q. Electro-Controlled Living Cationic Polymerization. *Angew. Chem. Int. Edit.* **2018**, *57* (18), 4907-4911.